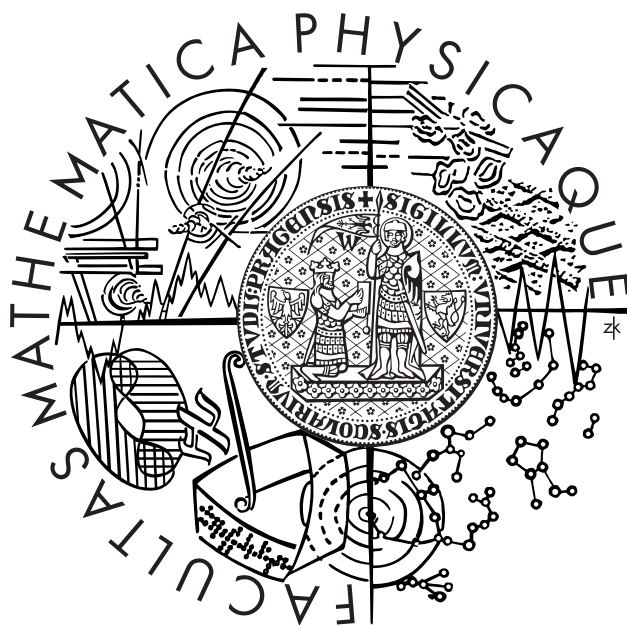


Charles University in Prague
Faculty of Mathematics and Physics

DIPLOMA THESIS



Petr Soukup

Electroweak processes in the framework of effective field theory

Institute of Particle and Nuclear Physics
Supervisor: RNDr. Karol Kampf, Ph.D.
Field of study: Theoretical physics

Acknowledgments

I would like to express my thanks to my supervisor, Dr. Karol Kampf and my adviser, Prof. Jiří Hořejší for their advice, help and support of my work. My gratitude also belongs to Dr. Jiří Novotný for his advice regarding the area of renormalization of effective field theories and his guidance in using Wolfram Mathematica software.

I hereby claim that I wrote my thesis entirely by myself, solely and only with the use of listed sources. I give my permission to make this work publicly available.

Prague, July 16, 2009

Petr Soukup

Contents

1	Introduction	6
2	Summary of the GWS Standard model	8
3	Standard model results	13
3.1	$H \rightarrow \gamma\gamma$ in Standard Model	13
4	Dimension-six effective operators	16
5	Electroweak processes within the effective field theory	19
5.1	$H \rightarrow \gamma\gamma$ decay at the tree level	19
5.2	$H \rightarrow \gamma\gamma$ decay at one-loop level	21
5.2.1	Contribution of the operator O_{WWW}	21
5.2.2	Contribution of the operator O_{WW}	26
5.2.3	Contribution of the operator O_W	33
5.2.4	Contribution of the operator O_{DW}	33
5.2.5	Contribution of the operator O_{BW}	34
5.2.6	Contribution of the operator O_{BB}	35
5.2.7	Contribution of the operator O_B	35
5.2.8	Contribution of operators $O_{DB}, O_{\Phi,1}, O_{\Phi,2}$ and $O_{\Phi,3}$	35
5.2.9	Overall contribution of dimension-six operators to $H \rightarrow \gamma\gamma$ process at one-loop level	36

CONTENTS

6 Renormalization	37
6.1 Renormalization in quantum field theories	37
6.2 Renormalization of $H \rightarrow \gamma\gamma$ at one-loop level	46
7 Reducible graphs	49
7.1 One-loop corrections to the external Higgs line	49
7.2 One-loop corrections to the external Photon line	58
7.3 One-loop vertex corrections	61
8 Discussion of results and conclusion	63
8.1 Summary of results and discussion	63
8.2 Conclusion	70
A Loop integrals	71

Název práce: *Elektroslabé procesy v rámci efektivní polní teorie*

Autor: *Petr Soukup*

Katedra (ústav): *Ústav částicové a jaderné fyziky*

Vedoucí diplomové práce: *RNDr. Karol Kampf, Ph.D.*

e-mail vedoucího: *kampf@troja.mff.cuni.cz*

Abstrakt: *V této práci studujeme elektroslabé procesy v rámci efektivní polní teorie za použití techniky efektivních Lagrangiánů, zejména proces rozpadu $H \rightarrow \gamma\gamma$. Je použita kompletní sada efektivních operátorů dimenze 6 invariantní vůči grupě $SU(2) \times U(1)$. Prezentujeme stručný úvod do GWS Standardního modelu a použitých operátorů dimenze 6. Pro proces $H \rightarrow \gamma\gamma$ je poté spočten příspěvek Standardního modelu na úrovni jedné smyčky a kompletní sada diagramů pocházející z efektivní teorie na stromové úrovni a na úrovni jedné smyčky. Následuje obecný stručný popis renormalizace v kvantové teorii pole. Pro spočtené procesy provedeme renormalizaci a diskutujeme obtíže při renormalizaci výpočtů v rámci nerenormalizovatelných teorií. Na závěr je provedena diskuze výsledků, zejména závislost rozpadové šířky $H \rightarrow \gamma\gamma$ na volných parametrech efektivní teorie a škále nové fyziky Λ . Provádíme diskuzi možných odchylek od Standardního modelu. Výsledky jsou znázorněny graficky.*

Klíčová slova: *Efektivní polní teorie, Elektroslabé procesy v rozšíření Standardního modelu, Efektivní lagrangiány, Lagrangiány dimenze 6, Rozpad $H \rightarrow \gamma\gamma$ ve fyzice za Standardním modelem, renormalizace nerenormalizovatelných teorií*

Title: *Electroweak processes in the framework of effective field theory*

Author: *Petr Soukup*

Department: *Institute of Particle and Nuclear Physics*

Supervisor: *RNDr. Karol Kampf, Ph.D.*

Supervisor's e-mail address: *kampf@troja.mff.cuni.cz*

Abstract: *In this thesis, we study electroweak processes within the framework of effective field theory employing the approach of effective Lagrangians. We mainly focus on the decay process $H \rightarrow \gamma\gamma$. A complete set of $SU(2) \times U(1)$ invariant dimension-six operators is utilized. We present a brief introduction to GWS Standard model and dimension-six effective operators. One-loop Standard model contribution to the process of $H \rightarrow \gamma\gamma$ is then evaluated, followed by calculation of tree-level and one-loop level dimension-six operators contribution to the same process. We then present a brief general summary of renormalization procedure in quantum field theory. Renormalization of performed calculations is implemented, and possible issues that may arise during renormalization of such non-renormalizable theory are also discussed. In the end, we discuss the obtained results, mainly the dependence of $H \rightarrow \gamma\gamma$ decay rate on effective theory's free parameters and the scale of the new physics Λ . Focus is made on possible deviations from Standard model results. The results are plotted in charts.*

Keywords: *Effective field theory, Electroweak processes within extension of Standard model, Effective Lagrangians, Dimension 6 Lagrangians, $H \rightarrow \gamma\gamma$ decay in physics beyond Standard Model, renormalization on non-renormalizable theories.*

Chapter 1

Introduction

The standard model (SM) of particle physics has been established as a very successful theory up to now. The most significant unresolved issue is the mechanism of the electroweak symmetry breaking and hypothetical existence of the so-called Higgs scalar sector. Current experiments seem to be supporting relatively light Higgs boson conjecture, i.e. $m_H < 200$ GeV (see [1]). However, today's general prevailing opinion is that SM cannot be for several reasons a final theory of particle physics, which means it should be perceived as an effective theory valid below the energy scale of certain magnitude - approximately 1 TeV - in accordance with today's experiments. Above this level, some new physics should emerge. For more details, see for example [2]. A general tool for describing the physics beyond SM is the approach of effective Lagrangians. This approach includes, besides common renormalizable interaction terms with the dimension three and four, also higher-dimensional terms that are not renormalizable. Such terms are scaled by negative power of Λ , the appropriate scale of the new physics. It follows that general form of such effective Lagrangian will be [3]:

$$\mathcal{L}_{\text{eff}} = \mathcal{L}_{SM} + \sum_{n \geq 5} \sum_{i=1}^{N_n} \frac{\alpha_i^{(n)}}{\Lambda^{n-4}} \mathcal{O}_i^{(n)}. \quad (1.1)$$

It is logical to keep the the $SU(2) \times U(1)$ invariance as a guiding principle when building up this extension of SM. We can also safely assume that $\Lambda \gg v$, where $v \doteq 246$ GeV is the common electroweak scale. This is in accordance with the so-called “decoupling scenario” where the $SU(2) \times U(1)$ symmetry is realized linearly (more details can be found e.g. in [3, 5]). What this means particularly is that the unphysical Goldstone boson appears through the standard complex $SU(2)$ doublet, together with the Higgs boson field and generally, the low-energy is identical with that of SM. For specific representation of the higher-order non-renormalizable $SU(2) \times U(1)$ invariant terms we refer to [8] and [9]. Contributions of the higher-dimensional terms is then suppressed by the powers of the ratio v/Λ

at low-energy processes. In upcoming experiments (e.g. LHC) that also involve a search for the Higgs particle, process $H \rightarrow \gamma\gamma$ could lead to the detection of Higgs particle in case of lower Higgs mass (i.e. $m_H < 2m_W$), and this could also be sensitive to the effects of new physics described by the Lagrangian (1.1).

Chapter 2

Summary of the GWS Standard model

Let us start with summing-up the electroweak standard model of elementary particles. We will present here only a brief draft for reference purposes. For full details, we refer to the book [6]. The electroweak standard model formulated by S. Glashow, S. Weinberg and A. Salam describes electromagnetic and weak interactions of elementary particles in a unified relativistic quantum field theory. It consists of:

- 3 generations of elementary spin 1/2 fermions (leptons and quarks)
- spin 1 bosons (W^\pm, Z^0) and photon
- spin 0 particle - the Higgs scalar boson H

The fermions are conventionally considered as the constituents of matter while the spin-1 bosons are thought to be the carriers of electroweak force, hence their name intermediate bosons. The Higgs boson, which has not been yet confirmed by experiment, is related to the mechanism of mass generation of the other particles.

The fundamental principle, that this model is based upon, is local $SU(2) \times U(1)$ gauge symmetry where W^\pm, Z^0 and photon are vector fields that consist of linear combinations of four original Yang-Mills fields associated with four $SU(2) \times U(1)$ generators. Basic building blocks of the fermion sector here are left-handed $SU(2)$ doublets:

$$\begin{aligned} L^{(e)} &= \begin{pmatrix} \nu_{eL} \\ e_L \end{pmatrix}, & L^{(\mu)} &= \begin{pmatrix} \nu_{\mu L} \\ \mu_L \end{pmatrix}, & L^{(\tau)} &= \begin{pmatrix} \nu_{\tau L} \\ \tau_L \end{pmatrix}, \\ L_0^{(d)} &= \begin{pmatrix} u_{0L} \\ d_{0L} \end{pmatrix}, & L_0^{(s)} &= \begin{pmatrix} c_{0L} \\ s_{0L} \end{pmatrix}, & L_0^{(b)} &= \begin{pmatrix} t_{0L} \\ b_{0L} \end{pmatrix}, \end{aligned} \quad (2.1)$$

and right-handed $SU(2)$ singlets:

$$e_R, \mu_R, \tau_R, d_{0R}, u_{0R}, s_{0R}, c_{0R}, b_{0R}, t_{0R}, \quad (2.2)$$

where the left and right components are obtained by the means of the projection operators:

$$e_L = \frac{1}{2}(1 - \gamma_5)e, \quad e_R = \frac{1}{2}(1 + \gamma_5)e$$

In order to implement the Higgs mechanism, we make a use of the $SU(2)$ doublet of complex scalar fields. Such doublet represents four real scalar fields. Three of these fields are would-be Goldstone bosons associated with spontaneously broken $SU(2)$ symmetry and can be eliminated by the means of so-called U -gauge which is equivalent to $SU(2)$ rotation within the Lagrangian. In U -gauge, the complex scalar doublet becomes

$$\Phi_U = \frac{1}{\sqrt{2}} \begin{pmatrix} 0 \\ v + H \end{pmatrix} \quad (2.3)$$

The GWS Lagrangian consists of four parts, namely

$$\mathcal{L}_{GWS} = \mathcal{L}_{gauge} + \mathcal{L}_{fermion} + \mathcal{L}_{Higgs} + \mathcal{L}_{Yukawa} \quad (2.4)$$

where \mathcal{L}_{gauge} is a pure Yang-Mills Lagrangian corresponding to the local symmetry $SU(2) \times U(1)$. The term $\mathcal{L}_{fermion}$ is composed of quark and lepton kinetic terms and their interactions with gauge fields. In its construction, we will make a use of doublets and singlets (2.1) and (2.2) along with the covariant derivative which we will adopt in the following form:

$$D_\mu = \partial_\mu + igT^a W_\mu^a + ig'Y B_\mu \quad (2.5)$$

W_μ^a and B_μ are the original Yang-Mills fields with

$$T^a = \frac{\sigma^a}{2} \quad (2.6)$$

where symbol σ means the standard Pauli matrices and

$$Q = T^3 + Y. \quad (2.7)$$

Q represents the electric charge in units of positron charge, Y is an arbitrary real parameter usually called the 'weak hypercharge', which is later constrained by the requirement of obtaining standard electromagnetic interactions of leptons carrying the usual electrical charges in the GWS Standard Model. Following relation holds:

$$T^3 = \begin{pmatrix} \frac{1}{2} & 0 \\ 0 & -\frac{1}{2} \end{pmatrix} \quad Y = \begin{pmatrix} \frac{1}{2} & 0 \\ 0 & \frac{1}{2} \end{pmatrix} \quad (2.8)$$

We shall proceed with the brief summary of steps that lead to the final form of GWS Lagrangian. Again, appropriate details can be found in [6].

- The original Yang-Mills gauge fields do not have any direct particle contents. They need to be mixed by the means of orthogonal transformation in order to describe the physical vector bosons.

$$B_\mu = -\sin\theta_W Z_\mu + \cos\theta_W A_\mu \quad (2.9)$$

$$W_\mu^3 = \cos\theta_W Z_\mu + \sin\theta_W A_\mu \quad (2.10)$$

$$W_\mu^1 = \frac{1}{\sqrt{2}}(W_\mu^+ + W_\mu^-) \quad (2.11)$$

$$W_\mu^2 = \frac{i}{\sqrt{2}}(W_\mu^+ - W_\mu^-) \quad (2.12)$$

where W_μ^+ , W_μ^- , Z_μ and A_μ represent the physical vector bosons.

Such a mixing is the source of the so-called “electroweak unification” within the GWS electroweak theory. The mixing parameter θ_W is called “weak mixing angle” or Weinberg angle. We also arrive here at the so-called “unification condition”, a relation between e and g coupling constants

$$e = g \sin\theta_W \quad (2.13)$$

- Next, through application of the Higgs mechanism in \mathcal{L}_{Higgs} , we generate the masses of W^\pm and Z bosons. During this process, the relation between massive bosons masses is established

$$m_W = m_Z \cos\theta_W \quad (2.14)$$

- We apply the Higgs mechanism in \mathcal{L}_{Yukawa} arriving at mass terms for charged leptons. Primordial fields (2.1) and (2.2) do not represent physical quarks, appropriate transformations have to be performed. Namely, through diagonalizing of 3×3 mass matrices for (2.1) and (2.2), masses for quarks are gained.
- Finally, through unitary rotations of primordial fields (2.1) and (2.2) in $\mathcal{L}_{fermion}$, we arrive at Cabbibo-Kobayashi-Maskawa (CKM) matrix which describes the interactions of weak charged currents.
- Let us also note that massive neutrinos and their eventual mixing could be also incorporated into SM construction by generalizing the technique used for quarks to the lepton sector, resulting in mass terms for neutrinos, Higgs boson interactions and lepton analogue of CKM matrix. However, for the purposes of this paper, we can ignore all that leaving neutrinos massless and ignoring their mixing as well.

The previous steps lead to the following form of electroweak SM Lagrangian:

$$\begin{aligned}
 \mathcal{L}_{int}^{GWS} = & \sum_f Q_f e \bar{f} \gamma^\mu f A_\mu + \mathcal{L}_{CC} + \mathcal{L}_{NC} \\
 & + ig(W_\mu^0 W_\nu^- \vec{\partial}^\mu W^{+\nu} + W_\mu^- W_\nu^+ \vec{\partial}^\mu W^{0\nu} + W_\mu^+ W_\nu^0 \vec{\partial}^\mu W^{-\nu}) \\
 & - g^2 \left[\frac{1}{2} (W^- \cdot W^+)^2 - \frac{1}{2} (W^-)^2 (W^+)^2 + (W^0)^2 (W^- \cdot W^+) \right. \\
 & \qquad \qquad \qquad \left. - (W^- \cdot W^0)(W^+ \cdot W^0) \right] \\
 & + gm_W W_\mu^- W^{+\mu} H + \frac{1}{2 \cos \theta_W} gm_Z Z_\mu Z^\mu H \\
 & + \frac{1}{4} g^2 W_\mu^- W^{+\mu} H^2 + \frac{1}{8} \frac{g^2}{\cos^2 \theta_W} Z_\mu Z^\mu H^2 \\
 & - \sum_f \frac{1}{2} g \frac{m_f}{m_W} \bar{f} f H - \frac{1}{4} g \frac{m_H^2}{m_W} H^3 - \frac{1}{32} g^2 \frac{m_H^2}{m_W^2} H^4, \tag{2.15}
 \end{aligned}$$

where the symbol $\vec{\partial}$ is defined as $f \vec{\partial}_\mu g = f(\partial_\mu g) - (\partial_\mu f)g$ and

$$W_\mu^0 = \cos \theta_W Z_\mu + \sin \theta_W A_\mu. \tag{2.16}$$

The charged weak boson fields are defined as

$$W_\mu^\pm = \frac{1}{\sqrt{2}} (W_\mu^1 \mp iW_\mu^2) \tag{2.17}$$

and the following relation also holds

$$G_F / \sqrt{2} = g^2 / (8m_W^2) \tag{2.18}$$

The charged current term \mathcal{L}_{CC} is given by

$$\begin{aligned}
 \mathcal{L}_{CC} = & \frac{g}{2\sqrt{2}} \sum_{\ell=e,\mu,\tau} \bar{\nu}_\ell \gamma^\lambda (1 - \gamma_5) \ell W_\lambda^+ \\
 & + \frac{g}{2\sqrt{2}} (\bar{u}, \bar{c}, \bar{t}) \gamma^\lambda (1 - \gamma_5) V_{CKM} \begin{pmatrix} d \\ s \\ b \end{pmatrix} W_\lambda^+ + h.c. \tag{2.19}
 \end{aligned}$$

where V_{CKM} stands for Cabbibo-Kobayashi-Maskawa 3×3 unitary matrix.

The term \mathcal{L}_{NC} reads as

$$\mathcal{L}_{NC} = \frac{g}{2 \cos \theta_W} \sum_f \bar{f} \gamma^\lambda (v_f - a_f \gamma_5) f Z_\lambda \tag{2.20}$$

with

$$v_f = -\frac{1}{2} - 2Q_f \sin^2 \theta_W \quad (2.21)$$

$$a_f = -\frac{1}{2}$$

for $f = e, \mu, \tau, d, s, b$ and

$$v_f = +\frac{1}{2} - 2Q_f \sin^2 \theta_W \quad (2.22)$$

$$a_f = +\frac{1}{2}$$

for $f = \nu_e, \nu_\mu, \nu_\tau, u, c, t$.

The mass of Higgs boson is given by

$$m_H^2 = 2\lambda v^2, \quad (2.23)$$

where the parameter v is related to the Fermi constant as

$$v = (G_F \sqrt{2})^{\frac{1}{2}} \doteq 246 \text{ GeV}. \quad (2.24)$$

Chapter 3

Standard model results

3.1 $H \rightarrow \gamma\gamma$ in Standard Model

We will begin our study of dimension-six bosonic operators by calculating $H \rightarrow \gamma\gamma$ decay process. Let us first look at the results given by the Standard Model, so we can later analyze dimension-six operators contribution and possible deviation from SM. Our starting point will be the electroweak SM Lagrangian (2.15.) It is a well known fact that SM does not contain any direct $H\gamma\gamma$ interaction. The reason is that the appropriate lowest-dimensional coupling would have to be of the form $HF_{\mu\nu}F^{\mu\nu}$. Such a term has the dimension five and thus cannot be present in a renormalizable Lagrangian. Therefore the leading contribution to the process $H \rightarrow \gamma\gamma$ in SM is given by one-loop diagrams. The most significant ones are represented by the top quark loop and W boson loop. The rest of the fermionic contributions is strongly suppressed due to the fact that Higgs-fermion interaction in Standard Model is proportional to the relevant fermion mass. The appropriate diagrams to be calculated are shown on Fig. 3.1.

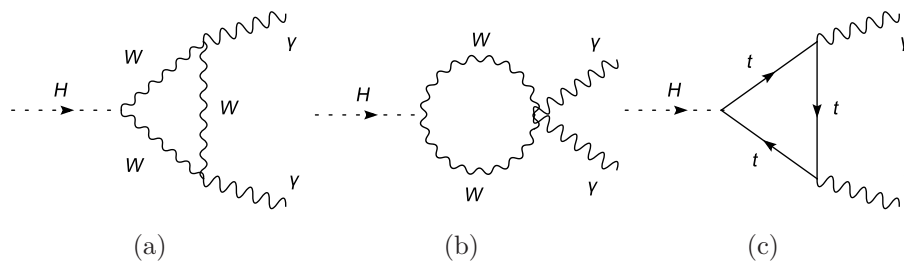


Figure 3.1: SM one-loop diagrams for $H \rightarrow \gamma\gamma$. Crossing of the external photon lines is automatically assumed for the graphs (a) and (c).

For graphs (a) and (b), we get the amplitudes:

$$\begin{aligned}
 i\mathcal{M}_{(a)} &= -e^2 g m_W \int \frac{d^4 l}{(2\pi)^4} \left[g^{\alpha\beta} \frac{-g^{\alpha\beta} + \frac{(l+p)^\alpha (l+p)^\beta}{m_W^2}}{(l+p)^2 - m_W^2} V_{\rho\beta\gamma}(p, -l-p, l) \right. \\
 &\quad \times \left. \frac{-g^{\gamma\delta} + \frac{l^\gamma l^\delta}{m_W^2}}{l^2 - m_W^2} V_{\sigma\delta\lambda}(k, -l, l-k) \frac{-g^{\lambda\iota} + \frac{(l-k)^\lambda (l-k)^\iota}{m_W^2}}{(l-k)^2 - m_W^2} \right] \\
 &\quad \times \varepsilon^{*\rho}(p) \varepsilon^{*\sigma}(k) \\
 i\mathcal{M}_{(b)} &= e^2 g m_W \int \frac{d^4 l}{(2\pi)^4} g^{\alpha\delta} \frac{-g^{\alpha\beta} + \frac{(l+p)^\alpha (l+p)^\beta}{m_W^2}}{(l+p)^2 - m_W^2} \frac{-g^{\gamma\delta} + \frac{(l-k)^\gamma (l-k)^\delta}{m_W^2}}{(l-k)^2 - m_W^2} \\
 &\quad \times (g^{\beta\sigma} g^{\gamma\rho} + g^{\beta\rho} g^{\gamma\sigma} - 2g^{\beta\gamma} g^{\rho\sigma}) \varepsilon^{*\rho}(p) \varepsilon^{*\sigma}(k)
 \end{aligned} \tag{3.1}$$

where $WW\gamma$ interaction is given by the function

$$V_{\lambda\mu\nu} = g_{\lambda\mu}(k-p)_\nu + g_{\mu\nu}(p-q)_\lambda + g_{\lambda\nu}(q-k)_\mu \tag{3.2}$$

with notation according to Fig. 3.2 and m_W represents the W boson mass.

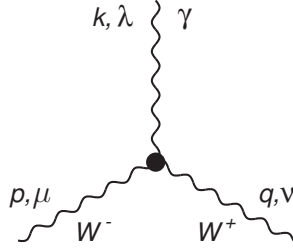


Figure 3.2: *SM vertex for $W^+W^-\gamma$ interaction. All impulses are taken as incoming.*

Loop-momentum integrals can be evaluated through the so-called Passarino-Veltman reduction, a method of reducing tensor one-loop integrals to special scalar integrals which can be further reduced to standard functions - namely logarithms and polylogarithms. For more details of this method we refer to Appendix A and also [13]. Explicit evaluations of these scalar integrals can be also found in Appendix A. Performing a straightforward evaluation of all the graphs in Fig. 3.1, we obtain a result for decay matrix element:

$$i\mathcal{M}_{\text{SM}} = e^2 g (F_{\text{VB}} + F_{\text{top}}) \left(g^{\mu\nu} - \frac{2k^\mu p^\nu}{m_H^2} \right) \varepsilon_\mu^*(p) \varepsilon_\nu^*(k) \tag{3.3}$$

where F_{VB} and F_{top} terms denote the contributions of the vector boson and top quark loops, respectively. They are expressed as

$$F_{\text{VB}} = \frac{3im_W}{8\pi^2} \left[1 + \frac{m_H^2}{6m_W^2} + (2m_W^2 - m_H^2) C_0(m_H^2, 0, 0, m_W^2, m_W^2, m_W^2) \right] \tag{3.4}$$

$$F_{\text{top}} = \frac{-i}{6\pi^2} \frac{m_t^2}{m_W} [2 + (4m_t^2 - m_H^2)C_0(m_H^2, 0, 0, m_t^2, m_t^2, m_t^2)] \quad (3.5)$$

with C_0 denoting the appropriate Passarino-Veltman function (see Appendix A). It is interesting to note that the following tensorial factor can be extracted in (3.3):

$$T^{\mu\nu} = g^{\mu\nu} - \frac{2k^\mu p^\nu}{m_H^2} \quad (3.6)$$

which is transverse with respect to the external photon momenta

$$p_\mu T^{\mu\nu} = 0, \quad k_\nu T^{\mu\nu} = 0. \quad (3.7)$$

Such transversality reflects the electromagnetic gauge invariance of the SM Lagrangian. The presence of this transverse factor will later also function as a significant ‘‘correction check’’ in subsequent calculations with the effective Lagrangian. It is also interesting to notice that matrix elements (6.4) are not transverse by themselves but only when they are summed together which is a fact that will become even more obvious in following calculations within the effective theory. The decay width is given by

$$\Gamma = \frac{1}{2} \frac{1}{16\pi m_H} |\mathcal{M}|^2 \quad (3.8)$$

where factor 1/2 is added because two identical particles in the final state are present. Substituting (3.3) into (3.8), we obtain the final expression for decay width of $H \rightarrow \gamma\gamma$ process:

$$\Gamma_{\text{SM}}(H \rightarrow \gamma\gamma) = \frac{8\pi\alpha^2 G_F m_W^2}{\sqrt{2} m_H} |F_{\text{top}} + F_{\text{VB}}|^2. \quad (3.9)$$

Chapter 4

Dimension-six effective operators

Let us now study in detail effective interactions with dimension greater than four. Looking back at the main scheme (1.1), it is apparent that the leading contribution of the new physics which has the appropriate structure for the $H \rightarrow \gamma\gamma$ process shall come from dimension-six operators. In this work, we are going to ignore dimension-six fermionic operators altogether. They have been previously studied in [7], and it turns out that their contribution is rather small compared to the dimension-six bosonic operators. So, as far as this work is concerned, we are going to effectively make those dimension-six fermionic coupling constants equal to zero: $f_i^{ferm} = 0$. Therefore the effective Lagrangian to work with will have the following form:

$$\mathcal{L}_{eff} = \mathcal{L}_{SM} + \sum_i \frac{f_i^{(6)}}{\Lambda^2} \mathcal{O}_{i(boson)}^{(6)}. \quad (4.1)$$

Adopting a realistic assumption that the bosonic sector of our effective low-energy theory contains only particles W^\pm , Z , γ and H , and also introducing $SU(2) \times U(1)$ gauge symmetry requirement, together with separate invariance under charge conjugation and parity, one arrives at the conclusion that there are exactly eleven dimension-six operators altogether that possess all such required properties. They are namely:

$$O_{WWW} = \text{Tr}[\hat{W}_{\mu\nu}\hat{W}^{\nu\rho}\hat{W}_\rho^\mu] \quad (4.2)$$

$$O_{WW} = \Phi^\dagger \hat{W}_{\mu\nu} \hat{W}^{\mu\nu} \Phi \quad (4.3)$$

$$O_{BW} = \Phi^\dagger \hat{W}_{\mu\nu} \hat{B}^{\mu\nu} \Phi \quad (4.4)$$

$$O_{DW} = \text{Tr}([D_\mu, \hat{W}_{\nu\rho}][D^\mu, \hat{W}^{\nu\rho}]) \quad (4.5)$$

$$O_{DB} = -\frac{g'^2}{2} (\partial_\mu B_{\nu\rho})(\partial^\mu B^{\nu\rho}) \quad (4.6)$$

$$O_{BB} = \Phi^\dagger \hat{B}_{\mu\nu} \hat{B}^{\mu\nu} \Phi \quad (4.7)$$

$$O_W = (D_\mu \Phi)^\dagger \hat{W}^{\mu\nu} (D_\nu \Phi) \quad (4.8)$$

$$O_B = (D_\mu \Phi)^\dagger \hat{B}^{\mu\nu} (D_\nu \Phi) \quad (4.9)$$

$$O_{\Phi,1} = (D_\mu \Phi)^\dagger \Phi^\dagger \Phi (D^\mu \Phi) \quad (4.10)$$

$$O_{\Phi,2} = \frac{1}{2} \partial^\mu (\Phi^\dagger \Phi) \partial_\mu (\Phi^\dagger \Phi) \quad (4.11)$$

$$O_{\Phi,3} = \frac{1}{3} (\Phi^\dagger \Phi)^3. \quad (4.12)$$

A full construction of these operators was done systematically in [8], we are giving here just a brief list.

Here, we denote

$$\hat{W}_{\mu\nu} = igT^a W_{\mu\nu}^a, \quad \hat{B}_{\mu\nu} = ig' B_{\mu\nu}. \quad (4.13)$$

The Higgs field is again introduced in U -gauge - see (2.3).

We will also introduce 2×2 matrices

$$T^\pm = T^1 \pm iT^2. \quad (4.14)$$

Relation (2.5) can be expressed with the help of (4.14), (2.11) and (2.12) as

$$D_\mu = \partial_\mu + i \frac{g}{\sqrt{2}} (W_\mu^+ T^+ + W_\mu^- T^-) + ig_Z (T^3 - \sin^2 \theta_W Q) Z_\mu + ie Q A_\mu. \quad (4.15)$$

Operators (4.2) through (4.12) can be quite easily expressed in a form suitable for formulation in terms of physical fields:

$$O_{WWW} = -i \frac{3}{2} g^3 W_{\mu\nu}^+ W^{-\nu\rho} W_\rho^3 \quad (4.16)$$

$$O_{WW} = -\frac{g^2}{2} (\Phi^\dagger \Phi) \left[W_{\mu\nu}^+ W^{-\mu\nu} + \frac{1}{2} W_{\mu\nu}^3 W^{3\mu\nu} \right] \quad (4.17)$$

$$\begin{aligned} O_{BW} = & -\frac{gg'}{4} \left[\sqrt{2} (\Phi^\dagger T^+ \Phi) W_{\mu\nu}^+ + \sqrt{2} (\Phi^\dagger T^- \Phi) W_{\mu\nu}^- \right. \\ & \left. + (\Phi^\dagger \sigma^3 \Phi) W_{\mu\nu}^3 \right] B^{\mu\nu} \end{aligned} \quad (4.18)$$

$$O_{DW} = -g^2 \left[(D_\mu W_{\nu\rho})^+ (D^\mu W^{\nu\rho})^- + \frac{1}{2} (D_\mu W_{\nu\rho})^3 (D^\mu W^{\nu\rho})^3 \right] \quad (4.19)$$

$$O_{DB} = -\frac{g'^2}{2}(\partial_\mu B_{\nu\rho})(\partial^\mu B^{\nu\rho}) \quad (4.20)$$

$$O_{BB} = -\frac{g'^2}{4}(\Phi^\dagger\Phi)B_{\mu\nu}B^{\mu\nu} \quad (4.21)$$

$$O_W = \frac{ig}{2}\left[\sqrt{2}(D^\mu\Phi)^\dagger T^+(D^\nu\Phi)W_{\mu\nu}^+ + \sqrt{2}(D^\mu\Phi)^\dagger T^-(D^\nu\Phi)W_{\mu\nu}^- + (D^\mu\Phi)^\dagger\sigma^3(D^\nu\Phi)W_{\mu\nu}^3\right] \quad (4.22)$$

$$O_B = \frac{ig'}{2}(D^\mu\Phi)^\dagger(D^\nu\Phi)B_{\mu\nu}, \quad (4.23)$$

where operators without carets are

$$W_{\mu\nu}^\pm = \partial_\mu W_\nu^\pm - \partial_\nu W_\mu^\pm \pm ig(W_\mu^3 W_\nu^\pm - W_\nu^3 W_\mu^\pm) \quad (4.24)$$

$$W_{\mu\nu}^3 = \partial_\mu W_\nu^3 - \partial_\nu W_\mu^3 + ig(W_\mu^+ W_\nu^- - W_\nu^+ W_\mu^-) \quad (4.25)$$

$$B_{\mu\nu} = \partial_\mu B_\nu - \partial_\nu B_\mu \quad (4.26)$$

$$(D_\mu W_{\nu\rho})^\pm = \partial_\mu W_{\nu\rho}^\pm \pm ig(W_\mu^3 W_{\nu\rho}^\pm - W_\mu^\pm W_{\nu\rho}^3) \quad (4.27)$$

$$(D_\mu W_{\nu\rho})^3 = \partial_\mu W_{\nu\rho}^3 + ig(W_\mu^+ W_{\nu\rho}^- - W_\mu^- W_{\nu\rho}^+). \quad (4.28)$$

(4.15) acting on (2.3) will yield:

$$D_\mu\Phi = \begin{pmatrix} \frac{ig}{2}W_\mu^+(v+H) \\ \frac{1}{\sqrt{2}}\left[\partial_\mu - \frac{ig_z Z_\mu}{2}\right](v+H) \end{pmatrix}. \quad (4.29)$$

Substituting (4.24) through (4.28) and (2.3) into (4.16) through (4.23), we finally obtain dimension-six operators expressed in the language of physical fields. These are quite long, and listing them here would take excessive amount of space.

Chapter 5

Electroweak processes within the effective field theory

5.1 $H \rightarrow \gamma\gamma$ decay at the tree level

As we have stated in the previous section, there is no direct $H\gamma\gamma$ interaction in Standard Model. However, dimension-six operators allow such interaction, so there will be non-trivial contribution to $H \rightarrow \gamma\gamma$ at the tree-level. Relevant operators here will be O_{WW} , O_{BW} and O_{BB} , the others will give zero contribution.

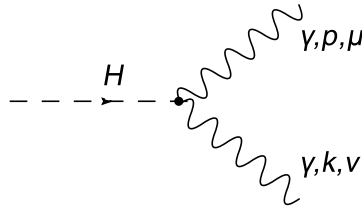


Figure 5.1: H to $\gamma\gamma$ decay at the tree level

Feynman rules corresponding to these operators and direct $H\gamma\gamma$ interaction will be:

$$V_{WW}^{tree} = -ivg^2 \sin^2 \theta_W (k^\mu p^\nu - g^{\mu\nu} k \cdot p) \quad (5.1)$$

$$V_{BB}^{tree} = -ivg'^2 \cos^2 \theta_W (k^\mu p^\nu - g^{\mu\nu} k \cdot p) \quad (5.2)$$

$$V_{BW}^{tree} = ivgg' \cos \theta_W \sin \theta_W (k^\mu p^\nu - g^{\mu\nu} k \cdot p) \quad (5.3)$$

The photon momenta here are taken as outgoing and the following relation holds:

$$e = g \sin \theta_W = g' \cos \theta_W. \quad (5.4)$$

The matrix element descending from this diagram will have quite simple form:

$$iM_{\text{eff}}^{\text{tree}}(H \rightarrow \gamma\gamma) = \frac{i}{2} m_H^2 v e^2 \left(\frac{f_{BB}}{\Lambda^2} - \frac{f_{BW}}{\Lambda^2} + \frac{f_{WW}}{\Lambda^2} \right) (g^{\mu\nu} - \frac{2k^\mu p^\nu}{m_H^2}) \varepsilon_\mu^*(p) \varepsilon_\nu^*(k). \quad (5.5)$$

We can also notice that it exhibits the desirable transverse tensor structure.

5.2 $H \rightarrow \gamma\gamma$ decay at one-loop level

Let us now proceed with calculation of one-loop graphs, namely one-particle irreducible one-loop graphs. These have been first calculated systematically in [3] and [4]. We are interested in obtaining the leading order $\sim O(1/\Lambda^2)$ graphs within the $\mathcal{L}_{\text{boson}}^{(6)}$ domain, which means we are going to consecutively replace all SM vertices in Fig 3.1 a,b with the effective ones originating from $\mathcal{L}_{\text{boson}}^{(6)}$, replacing one vertex at a time. In another words, we are seeking those diagrams in which a vertex coming from $\mathcal{L}_{\text{boson}}^{(6)}$ appears exactly once. Some of the dimension-six operators also contain the W^+W^- terms which are proportional to the vector boson kinetic terms. Such terms will be included in the considered Feynman graphs in a straight way within our calculation, i.e. as a regular dimension-six effective coupling, so we will get a modified effective propagator this way [3]. An alternative method of dealing with such terms would lie in incorporating these effects into renormalization constants of the SM. This approach is applied for example in [8]. Again, in order to keep at $O(1/\Lambda^2)$ level, we are going to insert one modified propagator with effective W^+W^- coupling at a time. It means, we are going to get 8 graphs with modified propagator - including the crossed ones - see Fig. 5.8. This way, 16 modified SM-like topologies will emerge (including the crossed diagrams). In addition, there are new topologies (i.e. not SM-like) that originate purely from $\mathcal{L}_{\text{boson}}^{(6)}$. We are going to get the following new non SM-like interactions: apart the already mentioned $H\gamma\gamma$, we will also obtain $HW^+W^-\gamma$, $HH\gamma\gamma$ and $HW^+W^-\gamma\gamma$ interactions. New topologies that resemble one-loop graphs with one $\mathcal{L}_{\text{boson}}^{(6)}$ interaction are pictured in Fig. 5.2. We get 5 of these new non SM-like topologies (including the crossed ones). So, it's 21 effective diagrams altogether we are going to calculate. It is also worthy to mention that effective propagators will be inserted only to SM-like graphs, since the new topologies in Fig. 5.2 already have one effective dimension-six coupling and therefore are already $O(1/\Lambda^2)$.

We shall now proceed with explicitly listing all the relevant contributions of each dimension-six operator one by one. We are going to discuss the operators individually for better clarity.

5.2.1 Contribution of the operator O_{WWW}

Considering the $H \rightarrow \gamma\gamma$ process at one loop level, the operator O_{WWW} has the following relevant interactions: $W^+W^-\gamma$ and $W^+W^-\gamma\gamma$. This operator thus does not give any contributions to the new topologies in Fig. 5.2, so we get just SM-like diagrams that are depicted in Fig. 5.3. Heavy dots represent the $\mathcal{L}_{\text{boson}}^{(6)}$ vertices. As mentioned before, we are inserting only one effective vertex at a time to stay at $O(1/\Lambda^2)$ level. This means that other vertices without dot in Fig. 5.3 are regular SM vertices originating from (2.15) Lagrangian.

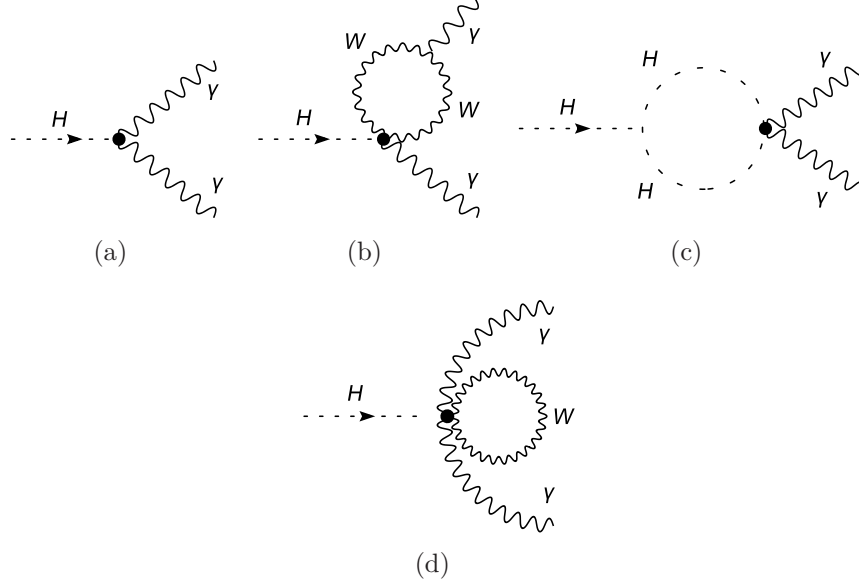


Figure 5.2: *Effective graphs with other than SM-like topologies. Heavy dots represent dimension-six effective vertices. Presence of the crossed graph in case of (b) is tacitly assumed.*

For $W^+W^-\gamma$ and $W^+W^-\gamma\gamma$ vertices, we get the following Feynman rules:

$$\begin{aligned}
 V_{O_{WW\gamma}}^{WW\gamma} = & -\frac{3}{2}ig^3 \sin(\theta_w) f_{WWW} \left[p^\lambda q^\mu k^\nu - q^\lambda k^\mu p^\nu + g^{\mu\nu} (q^\lambda k \cdot p - p^\lambda k \cdot q) \right. \\
 & \left. - g^{\lambda\nu} (q^\mu k \cdot p - k^\mu p \cdot q) + g^{\lambda\mu} (p^\nu k \cdot q - k^\nu p \cdot q) \right] \quad (5.6)
 \end{aligned}$$

$$\begin{aligned}
 V_{O_{WW\gamma\gamma}}^{WW\gamma\gamma} = & \frac{3}{2}ig^4 \sin^2(\theta_w) f_{WWW} \left[(r^\lambda q^\mu + q^\lambda (k^\mu - r^\mu) + p^\lambda r^\mu) g^{\nu\rho} - g^{\lambda\mu} (k \cdot q + p \cdot r) g^{\nu\rho} \right. \\
 & + g^{\mu\rho} (r^\lambda p^\nu + p^\lambda (k^\nu - r^\nu) + q^\lambda r^\nu) - g^{\lambda\rho} \left((k^\mu + r^\mu) p^\nu + q^\mu (k^\nu + r^\nu) \right) \\
 & + g^{\lambda\nu} \left(q^\mu k^\rho + k^\mu (p^\rho - q^\rho) + r^\mu q^\rho \right) + g^{\lambda\mu} \left(p^\nu k^\rho + r^\nu p^\rho + k^\nu (q^\rho - p^\rho) \right) \\
 & - g^{\mu\nu} (p^\lambda k^\rho + q^\lambda k^\rho + r^\lambda (p^\rho + q^\rho)) - g^{\lambda\nu} g^{\mu\rho} (k \cdot p + q \cdot r) \\
 & \left. + g^{\lambda\rho} g^{\mu\nu} (k \cdot p + k \cdot q + p \cdot r + q \cdot r) \right]. \quad (5.7)
 \end{aligned}$$

Impulse and index notation is given on Fig. 5.4.

It is now also convenient to recall that the incoming W^+ is equal to the outgoing W^- with the opposite impulse sign.

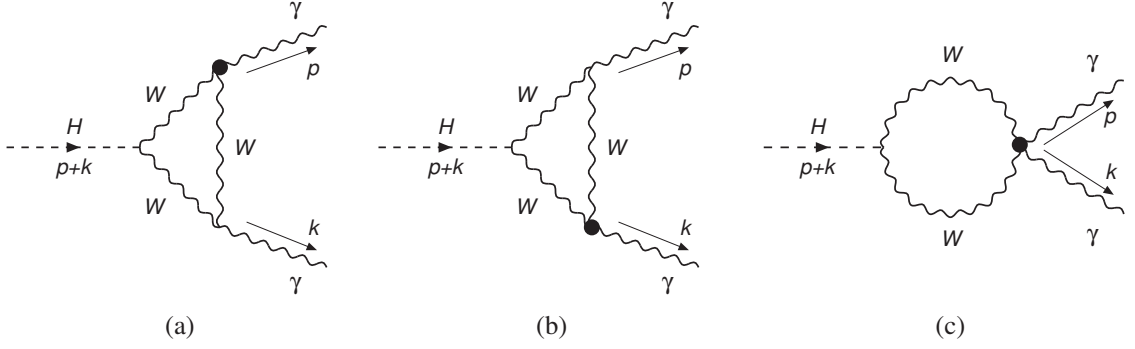


Figure 5.3: Operator O_{WWW} contributes to these effective graphs. Crossing of the external photon lines is tacitly assumed for the graphs (a) and (b).

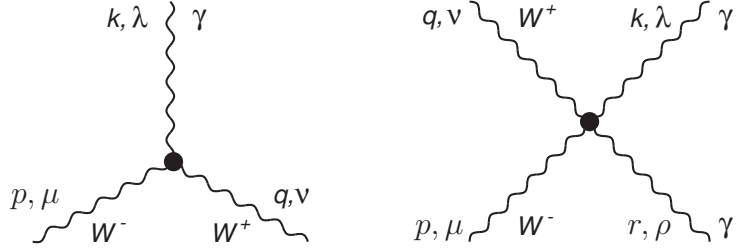


Figure 5.4: Effective vertices for $W^+W^-\gamma$ and $W^+W^-\gamma\gamma$ interactions. All impulses are taken as incoming.

For graphs (a) and (c), we get these amplitudes (it is obvious that (b) will be the same as (a) due to symmetry):

$$\begin{aligned}
 i\mathcal{M}_{O_{WWW}(a)} &= -\frac{3}{2} g^5 m_W \sin^2(\theta_W) f_{WWW} \int \frac{d^4l}{(2\pi)^4} \left[\frac{1}{[l^2 - m_W^2]} \frac{1}{[(l-k)^2 - m_W^2]} \right. \\
 &\quad \times \frac{1}{[(l+p)^2 - m_W^2]} g^{\alpha\epsilon} \left(\frac{(l^\alpha + p^\alpha)(l^\beta + p^\beta)}{m_W^2} - g^{\alpha\beta} \right) \\
 &\quad \times \left(\frac{l^\gamma l^\delta}{m_W^2} - g^{\gamma\delta} \right) \left(\frac{(l^\epsilon - k^\epsilon)(l^\phi - k^\phi)}{m_W^2} - g^{\phi\epsilon} \right) \\
 &\quad \times (g^{\sigma\phi}(l^\delta - 2k^\delta) + g^{\delta\phi}(k^\sigma - 2l^\sigma) + g^{\sigma\delta}(k^\phi + l^\phi)) \\
 &\quad \times (p^\beta l^\gamma l^\rho - l^\beta p^\gamma l^\rho + p^\beta p^\gamma l^\rho - l^\beta p^\gamma p^\rho + g^{\beta\rho}(p^\gamma l^2 - l^\gamma l \cdot p) \\
 &\quad \times -g^{\gamma\rho}(p^\beta l^2 - l^\beta l \cdot p + p^\beta l \cdot p - l^\beta p^2)
 \end{aligned}$$

$$\left. \times + g^{\beta\gamma} (p^\rho l \cdot p - l^\rho p^2) \right) \varepsilon^{*\rho}(p) \varepsilon^{*\sigma}(k), \quad (5.8)$$

$$\begin{aligned} i\mathcal{M}_{O_{WWW}(c)} &= \frac{3}{2} g^5 m_W \sin^2(\theta_W) f_{WWW} \int \frac{d^4 l}{(2\pi)^4} \frac{1}{[l^2 - m_W^2]} \frac{1}{[(k+l+p)^2 - m_W^2]} \\ &\times g^{\alpha\epsilon} \left(\frac{(k^\alpha + l^\alpha + p^\alpha)(k^\beta + l^\beta + p^\beta)}{m_W^2} - g^{\alpha\beta} \right) \left(\frac{l^\gamma l^\epsilon}{m_W^2} - g^{\gamma\epsilon} \right) \\ &\times \left((-l^\beta (k^\gamma + p^\gamma) + k^\beta (k^\gamma + l^\gamma + p^\gamma) + p^\beta (k^\gamma + l^\gamma + p^\gamma)) g^{\rho\sigma} \right. \\ &- g^{\beta\gamma} (k^2 + 2k \cdot p + p^2) g^{\rho\sigma} - g^{\beta\sigma} (l^\gamma k^\rho + p^\gamma (2k^\rho + l^\rho + p^\rho) \\ &- k^\gamma (2l^\rho + p^\rho)) - g^{\gamma\sigma} (-l^\beta k^\rho - p^\beta l^\rho + k^\beta (k^\rho + 2l^\rho + p^\rho)) \\ &- g^{\gamma\rho} (-k^\beta l^\sigma - l^\beta p^\sigma + p^\beta (k^\sigma + 2l^\sigma + p^\sigma)) \\ &- g^{\beta\rho} (-p^\gamma (k^\sigma + 2l^\sigma) + l^\gamma p^\sigma + k^\gamma (k^\sigma + l^\sigma + 2p^\sigma)) \\ &+ g^{\beta\rho} g^{\gamma\sigma} (k^2 + k \cdot l + k \cdot p - l \cdot p) + g^{\beta\gamma} (p^\rho p^\sigma + k^\rho (k^\sigma + 2p^\sigma)) \\ &\left. - g^{\beta\sigma} g^{\gamma\rho} (k \cdot l - k \cdot p - l \cdot p - p^2) \right) \varepsilon^{*\rho}(p) \varepsilon^{*\sigma}(k). \quad (5.9) \end{aligned}$$

These amplitudes can be evaluated in the similar matter as those in Chapter 3. We will also utilize apparent kinematic relations

$$p^2 = k^2 = 0 \quad (5.10)$$

$$p \cdot k = \frac{m_H^2}{2} \quad (5.11)$$

and momentum-polarization vector transversality

$$k^\mu \varepsilon_\mu(k) = 0. \quad (5.12)$$

Evaluation of (5.8) and (5.9) will yield results in terms of Passarino-Veltman scalar functions:

$$\begin{aligned}
 i \mathcal{F}_{O_{WWW(a+b)}} &= -\frac{ig^5}{96 m_W \pi^2} \sin^2(\theta_W) f_{WWW} \left(36C_0(m_H^2, 0, 0, m_W^2, m_W^2, m_W^2) m_W^4 \right. \\
 &\quad + 24B_0(0, m_W^2, m_W^2) m_W^2 - 18m_W^2 + m_H^2 \\
 &\quad \left. - 3(m_H^2 - 10m_W^2) B_0(m_H^2, m_W^2, m_W^2) \right) \\
 &\quad \times (m_H^2 g^{\rho\sigma} - 2k^\rho p^\sigma) \varepsilon^{*\rho}(p) \varepsilon^{*\sigma}(k), \tag{5.13}
 \end{aligned}$$

$$\begin{aligned}
 i \mathcal{F}_{O_{WWW(c)}} &= \frac{ig^5}{96 m_W \pi^2} \sin^2(\theta_W) f_{WWW} \left(m_H^2 + 6m_W^2 B_0(0, m_W^2, m_W^2) \right. \\
 &\quad \left. - 3(m_H^2 + 2m_W^2) B_0(m_H^2, m_W^2, m_W^2) \right) \\
 &\quad \times (m_H^2 g^{\rho\sigma} - 2k^\rho p^\sigma) \varepsilon^{*\rho}(p) \varepsilon^{*\sigma}(k). \tag{5.14}
 \end{aligned}$$

It is interesting to notice here that all three amplitudes have the transverse structure - again common factor $(m_H^2 g^{\rho\sigma} - 2k^\rho p^\sigma)$ which is transverse with respect to the external photon momenta can be pinpointed. Such occurrence is neither automatic, nor required. We only require that all the graphs originating from $\mathcal{L}_{\text{boson}}^{(6)}$, when summed together, have this transverse structure in order to reflect the electromagnetic gauge invariance of the Lagrangian. Thus, transversality of individual graphs is pure coincidence and does not occur all the time as we will see in some particular cases later on.

Summing together (5.13) and (5.14) we arrive at the final result for dimension-six operator O_{WWW} :

$$\begin{aligned}
 i \mathcal{F}_{O_{WWW}} &= -\frac{3ie^2 g^3}{16\pi^2} m_W f_{WWW} \left(2C_0(m_H^2, 0, 0, m_W^2, m_W^2, m_W^2) m_W^2 \right. \\
 &\quad \left. + B_0(0, m_W^2, m_W^2) + 2B_0(m_H^2, m_W^2, m_W^2) - 1 \right) \\
 &\quad \times (m_H^2 g^{\rho\sigma} - 2k^\rho p^\sigma) \varepsilon^{*\rho}(p) \varepsilon^{*\sigma}(k). \tag{5.15}
 \end{aligned}$$

We shall now continue with the contribution of the next dimension-six operator.

5.2.2 Contribution of the operator O_{WW}

This operator gives us some new graphs in addition to the previous one. Apart from $W^+W^-\gamma$ and $W^+W^-\gamma\gamma$ interactions, we are going to get SM-like dimension-six effective interaction W^+W^-H . We will also obtain the following non SM-like interactions that will give rise to the new topologies: $HW^+W^-\gamma$, $HH\gamma\gamma$ and $HW^+W^-\gamma\gamma$. And finally, we are getting dimension-six effective interaction W^+W^- terms. As we mentioned before, such terms will be included in the considered Feynman graphs as a regular dimension-six effective coupling.

Feynman rules originating from the operator O_{WW} will be as follows:

$$V_{O_{WW}}^{WW\gamma}(\lambda, \mu, \nu, k, p, q) = -2i e m_w^2 f_{WW} \left((p^\lambda - q^\lambda) g^{\mu\nu} - g^{\lambda\nu} (k^\mu - q^\mu) + g^{\lambda\mu} (k^\nu - p^\nu) \right) \quad (5.16)$$

$$V_{O_{WW}}^{WW\gamma\gamma}(\lambda, \rho, \mu, \nu, k, r, p, q) = 2i e^2 m_w^2 f_{WW} \times (-2g^{\lambda\rho} g^{\mu\nu} + g^{\lambda\nu} g^{\mu\rho} + g^{\lambda\mu} g^{\nu\rho}) \quad (5.17)$$

$$V_{O_{WW}}^{WWH}(\mu, \nu, p, q) = -2i g m_w f_{WW} (q^\mu p^\nu - g^{\mu\nu} p \cdot q). \quad (5.18)$$

The notation here is the same as in the case of previous operator - see Fig. 5.4. The notation for W^+W^-H is given on Fig. 5.5.

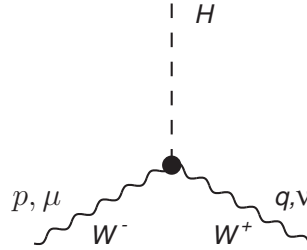


Figure 5.5: Effective vertex for W^+W^-H interaction. All impulses are taken as incoming.

Feynman rules for the new topologies/non SM-like interactions in case of O_{WW} will be quite simple:

$$V_{O_{WW}}^{HWW\gamma}(\lambda, \mu, \nu, k, p, q) = -2i e g m_w f_{WW} \left((p^\lambda - q^\lambda) g^{\mu\nu} - g^{\lambda\nu} (k^\mu - q^\mu) + g^{\lambda\mu} (k^\nu - p^\nu) \right) \quad (5.19)$$

$$V_{O_{WW}}^{HH\gamma\gamma}(\lambda, \rho, k, r) = i e^2 f_{WW} (g^{\lambda\rho} k \cdot r - r^\lambda k^\rho) \quad (5.20)$$

$$\begin{aligned}
 V_{O_{WW}}^{HWW\gamma\gamma}(\lambda, \rho, \mu, \nu, k, r, p, q) &= 2i e^2 g m_w f_{ww} \\
 &\times (-2g^{\lambda\rho} g^{\mu\nu} + g^{\lambda\nu} g^{\mu\rho} + g^{\lambda\mu} g^{\nu\rho}). \quad (5.21)
 \end{aligned}$$

Impulse and index notation for (5.19), (5.20) and (5.21) is according to Fig. 5.6.

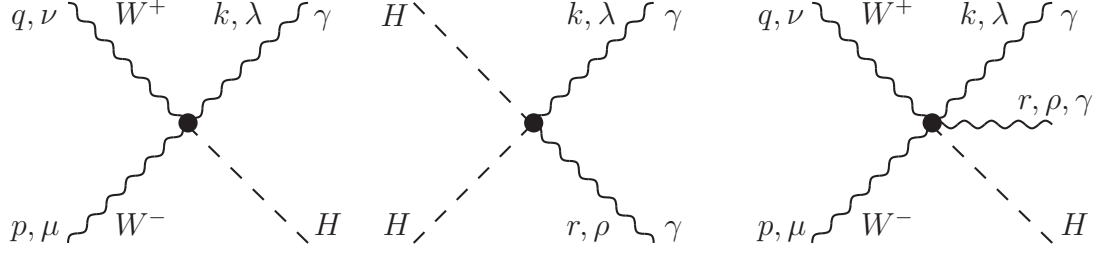


Figure 5.6: Effective vertices for $HW^+W^-\gamma$, $HH\gamma\gamma$ and $HW^+W^-\gamma\gamma$ interactions. All impulses are taken as incoming.

Finally, for the kinetic term/ W^+W^- interaction, we get:

$$V_{O_{WW}}^{WW} = -2i m_w^2 f_{ww} (q^\mu p^\nu - g^{\mu\nu} p \cdot q). \quad (5.22)$$

New topologies can be seen on Fig. 5.2. Writing down initial loop-momentum integrals for SM-like graphs is straightforward, so we will just mention here explicitly the new topologies. They correspond to the graphs (b), (c) and (d) on Fig. 5.2, respectively:

$$\begin{aligned}
 i\mathcal{M}_{O_{WW}}^{NT(b)} &= \frac{e^2 g}{8m_w^3 \pi^4} f_{ww} \int \frac{d^4 l}{(2\pi)^4} \frac{1}{[l^2 - m_w^2]} \frac{1}{[(l+p)^2 - m_w^2]} \\
 &\times (m_w^2 g^{\alpha\beta} - (l^\alpha + p^\alpha)(l^\beta + p^\beta)) \\
 &\times (m_w^2 g^{\gamma\delta} - l^\gamma l^\delta) (g^{\rho\gamma}(l^\beta - p^\beta + g^{\rho\beta}(l^\gamma + 2p^\gamma)) - g^{\beta\gamma}(2l^\rho + p^\rho)) \\
 &\times (k^\alpha g^{\delta\sigma} + l^\alpha g^{\delta\sigma} - g^{\alpha\sigma} k^\delta + g^{\alpha\sigma} l^\delta + g^{\alpha\sigma} p^\delta - 2g^{\alpha\delta} l^\sigma - g^{\alpha\delta} p^\sigma) \\
 &\times \varepsilon^{*\rho}(p) \varepsilon^{*\sigma}(k) \quad (5.23)
 \end{aligned}$$



Figure 5.7: Effective vertex for W^+W^- interaction. All impulses are taken as incoming.

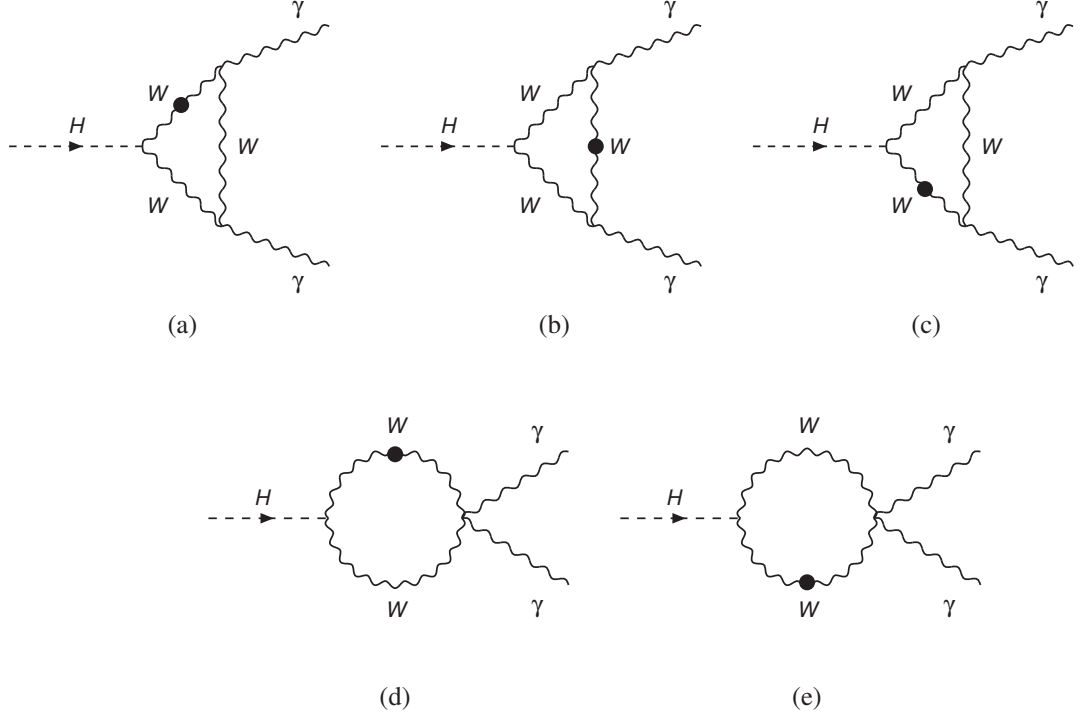


Figure 5.8: Propagators modified by dimension-six coupling in case of $H \rightarrow \gamma\gamma$ process. Crossing of the external photon lines is tacitly assumed for the graphs (a), (b) and (c).

$$\begin{aligned}
 i\mathcal{M}_{O_{WW}}^{NT(c)} &= \frac{3e^2g}{64m_W\pi^4 m_H^2} f_{WW} \int \frac{d^4l}{(2\pi)^4} \frac{1}{[l^2 - mh^2]} \frac{1}{[(k+l+p)^2 - mh^2]} \\
 &\times (k^\rho p^\sigma - g^{\rho\sigma} k \cdot p) \varepsilon^{*\rho}(p) \varepsilon^{*\sigma}(k)
 \end{aligned} \tag{5.24}$$

$$\begin{aligned}
 i\mathcal{M}_{O_{WW}}^{NT(d)} &= \frac{e^2g}{8m_W\pi^4} f_{WW} \int \frac{d^4l}{(2\pi)^4} \frac{1}{[l^2 - m_W^2]} (m_W^2 g^{\alpha\beta} - l^\alpha l^\beta) \\
 &\times (g^{\alpha\sigma} g^{\beta\rho} + g^{\alpha\rho} g^{\beta\sigma} - 2g^{\alpha\beta} g^{\rho\sigma}) \varepsilon^{*\rho}(p) \varepsilon^{*\sigma}(k)
 \end{aligned} \tag{5.25}$$

Graphs with effective dimension-six WW coupling are shown on Fig.5.8, we present here initial loop-momentum integral for graph (a):

$$\begin{aligned}
 i\mathcal{M}_{O_{WW}}^{EffProp(a)} &= \frac{e^2g m_W^3}{8\pi^4} f_{WW} \int \frac{d^4l}{(2\pi)^4} \frac{1}{[l^2 - m_W^2]} \frac{1}{[(l-k)^2 - m_W^2]} \frac{1}{[(l+p)^2 - m_W^2]^2} \\
 &\times g^{\alpha\epsilon} \left(\frac{l^\gamma l^\delta}{m_W^2} - g^{\gamma\delta} \right) \left(\frac{(l^\alpha + p^\alpha)(l^\lambda + p^\lambda)}{m_W^2} - g^{\alpha\lambda} \right) \left(\frac{(l^\beta + p^\beta)(l^\mu + p^\mu)}{m_W^2} - g^{\mu\beta} \right) \\
 &\times (g^{\rho\gamma}(l^\beta - p^\beta) + g^{\rho\beta}(l^\gamma + 2p^\gamma) + g^{\beta\gamma}(-2l^\rho - p^\rho)) \left(\frac{(l^\epsilon - k^\epsilon)(l^\phi - k^\phi)}{m_W^2} - g^{\phi\epsilon} \right) \\
 &\times (g^{\sigma\phi}(l^\delta - 2k^\delta) + g^{\delta\phi}(k^\sigma - 2l^\sigma) + g^{\sigma\delta}(k^\phi + l^\phi))
 \end{aligned}$$

$$\times \left(l^\lambda l^\mu + p^\lambda l^\mu + l^\lambda p^\mu + p^\lambda p^\mu - g^{\lambda\mu} (l+p)^2 \right) \varepsilon^{*\rho}(p) \varepsilon^{*\sigma}(k). \quad (5.26)$$

Evaluation of loop integrals will give us results in terms of Passarino-Veltman functions:

$$\begin{aligned} i \mathcal{F}_{O_{WW}}^{(a+b)} &= \frac{i e^2 g}{144 m_H^2 m_W \pi^2} f_{WW} \left(\left(432 C_0(m_H^2, 0, 0, m_W^2, m_W^2, m_W^2) m_W^6 \right. \right. \\ &\quad - 216 m_H^2 C_0(m_H^2, 0, 0, m_W^2, m_W^2, m_W^2) m_W^4 + 225 m_W^4 + 14 m_H^2 m_W^2 - 2 m_H^4 \\ &\quad - 6(m_W^4 + 5 m_H^2 m_W^2) B_0(0, m_W^2, m_W^2) + 3(5 m_H^4 - 22 m_W^2 m_H^2 + 56 m_W^4) \\ &\quad \times B_0(m_H^2, m_W^2, m_W^2) \Big) g^{\rho\sigma} m_H^2 + 2 \left(-432 C_0(m_H^2, 0, 0, m_W^2, m_W^2, m_W^2) m_W^6 \right. \\ &\quad + 216 m_H^2 C_0(m_H^2, 0, 0, m_W^2, m_W^2, m_W^2) m_W^4 - 216 m_W^4 - 34 m_H^2 m_W^2 \\ &\quad + 6(m_H^2 + 2 m_W^2) B_0(0, m_W^2, m_W^2) m_W^2 + m_H^4 \\ &\quad \left. \left. - 3(m_H^4 - 8 m_W^2 m_H^2 + 4 m_W^4) B_0(m_H^2, m_W^2, m_W^2) \right) k^\rho p^\sigma \right) \varepsilon^{*\rho}(p) \varepsilon^{*\sigma}(k) \quad (5.27) \end{aligned}$$

$$\begin{aligned} i \mathcal{F}_{O_{WW}}^{(c)} &= -\frac{i e^2 g}{288 m_H^2 m_W \pi^2} f_{WW} \left(\left(-2 m_H^4 - 22 m_W^2 m_H^2 + 9 m_W^4 - 6(m_W^4 + 5 m_H^2 m_W^2) \right. \right. \\ &\quad \times B_0(0, m_W^2, m_W^2) + 3(5 m_H^4 - 22 m_W^2 m_H^2 + 56 m_W^4) B_0(m_H^2, m_W^2, m_W^2) \Big) g^{\rho\sigma} m_H^2 \\ &\quad + 2 \left(m_H^4 + 2 m_W^2 m_H^2 + 6 m_W^2 (m_H^2 + 2 m_W^2) B_0(0, m_W^2, m_W^2) \right. \\ &\quad \left. \left. - 3(m_H^4 - 8 m_W^2 m_H^2 + 4 m_W^4) B_0(m_H^2, m_W^2, m_W^2) \right) k^\rho p^\sigma \right) \varepsilon^{*\rho}(p) \varepsilon^{*\sigma}(k) \quad (5.28) \end{aligned}$$

$$\begin{aligned} i \mathcal{F}_{O_{WW}}^{(e)} &= \frac{i e^2 g m_W}{144 m_H^2 \pi^2} f_{WW} \left(\left(-2 m_H^2 + 90 m_W^2 + 78 m_W^2 B_0(0, m_W^2, m_W^2) + (84 m_W^2 - 39 m_H^2) \right. \right. \\ &\quad \times B_0(m_H^2, m_W^2, m_W^2) \Big) g^{\rho\sigma} m_H^2 + 2 \left(m_H^2 + 6 m_W^2 B_0(0, m_W^2, m_W^2) \right. \\ &\quad \left. \left. - 3(m_H^2 + 2 m_W^2) B_0(m_H^2, m_W^2, m_W^2) \right) k^\rho p^\sigma \right) \varepsilon^{*\rho}(p) \varepsilon^{*\sigma}(k) \quad (5.29) \end{aligned}$$

$$\begin{aligned} i \mathcal{F}_{O_{WW}}^{(d)} &= -\frac{i e^2 g}{288 m_H^2 \pi^2} m_W f_{WW} \left(m_H^2 \left(72 C_0(m_H^2, 0, 0, m_W^2, m_W^2, m_W^2) m_H^4 \right. \right. \\ &\quad - 288 m_W^2 C_0(m_H^2, 0, 0, m_W^2, m_W^2, m_W^2) m_H^2 + 32 m_H^2 + 567 m_W^2 \\ &\quad - 6(18 m_H^2 - 53 m_W^2) B_0(0, m_W^2, m_W^2) + (168 m_W^2 - 78 m_H^2) B_0(m_H^2, m_W^2, m_W^2) \\ &\quad + 432 m_W^4 C_0(m_H^2, 0, 0, m_W^2, m_W^2, m_W^2) \Big) g^{\rho\sigma} - 4 \left(36 C_0(m_H^2, 0, 0, m_W^2, m_W^2, m_W^2) m_H^4 \right. \\ &\quad \left. \left. - 144 m_W^2 C_0(m_H^2, 0, 0, m_W^2, m_W^2, m_W^2) m_H^2 + 17 m_H^2 + 108 m_W^2 \right. \right. \end{aligned}$$

$$\begin{aligned}
 & -6 (9m_H^2 + m_W^2) B_0 (0, m_W^2, m_W^2) + 3 (m_H^2 + 2m_W^2) B_0 (m_H^2, m_W^2, m_W^2) \\
 & + 216 m_W^4 C_0 (m_H^2, 0, 0, m_W^2, m_W^2, m_W^2) \Big) k^\rho p^\sigma \Big) \varepsilon^{*\rho}(p) \varepsilon^{*\sigma}(k), \tag{5.30}
 \end{aligned}$$

where letters (a), (b), (c), (d) and (e) denote the results for graphs according to the Fig. 5.9.

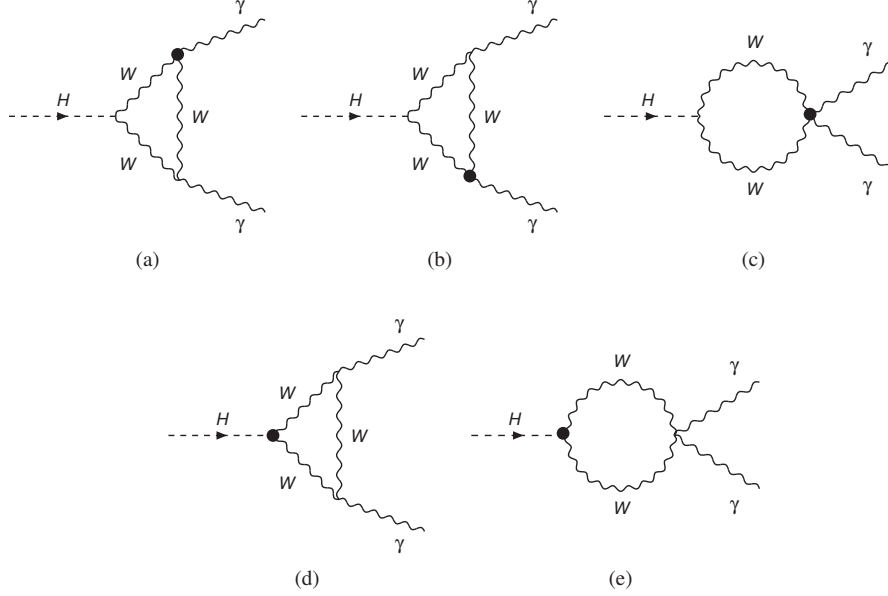


Figure 5.9: Letter symbols for SM-like topologies in $H \rightarrow \gamma\gamma$ process

Calculating loop integrals for the new topologies will give us results:

$$\begin{aligned}
 i \mathcal{F}_{O_{WW}}^{NT(b)} &= \frac{i e^2 g m_W}{16 \pi^2} f_{WW} \left(\left(2 m_H^2 + 19 m_W^2 - 6 (m_H^2 - 3 m_W^2) \right. \right. \\
 & \quad \times B_0 (0, m_W^2, m_W^2) \Big) g^{\rho\sigma} + 4 (3 B_0 (0, m_W^2, m_W^2) - 1) k^\rho p^\sigma \Big) \\
 & \quad \times \varepsilon^{*\rho}(p) \varepsilon^{*\sigma}(k) \tag{5.31}
 \end{aligned}$$

$$\begin{aligned}
 i \mathcal{F}_{O_{WW}}^{NT(c)} &= - \frac{3 i e^2 g m_H^2 f_{WW} B_0 (m_H^2, m_H^2, m_H^2) (m_H^2 g^{\rho\sigma} - 2 k^\rho p^\sigma)}{128 m_W \pi^2} \\
 & \quad \times \varepsilon^{*\rho}(p) \varepsilon^{*\sigma}(k) \tag{5.32}
 \end{aligned}$$

$$i \mathcal{F}_{O_{WW}}^{NT(d)} = - \frac{i e^2 g m_W^3 f_{WW} (18 B_0 (0, m_W^2, m_W^2) + 19) g^{\rho\sigma}}{32 \pi^2} \varepsilon^{*\rho}(p) \varepsilon^{*\sigma}(k), \tag{5.33}$$

where letter symbols (b), (c) and (d) denote graphs according to Fig. 5.2.

Let us proceed with evaluating the loops with dimension-six WW couplings:

$$\begin{aligned}
 i\mathcal{F}_{O_{WW}}^{EffProp(a)} = & -\frac{ie^2g}{576m_H^4\pi^2}f_{WW}m_W\left(m_H^4\left(1728D_0(m_H^2,m_H^2,0,0,0,0,m_W^2,m_W^2,m_W^2,m_W^2)m_W^6\right.\right. \\
 & + 864C_0(m_H^2,0,0,m_W^2,m_W^2,m_W^2)m_W^4 + 792C_0(m_H^2,m_H^2,0,m_W^2,m_W^2,m_W^2)m_W^4 \\
 & - 288m_H^2D_0(m_H^2,m_H^2,0,0,0,0,m_W^2,m_W^2,m_W^2,m_W^2)m_W^4 \\
 & - 360m_H^2C_0(m_H^2,0,0,m_W^2,m_W^2,m_W^2)m_W^2 - 54m_H^2C_0(m_H^2,m_H^2,0,m_W^2,m_W^2,m_W^2)m_W^2 \\
 & + 396m_W^2 + 50m_H^2 - 3(9m_H^2 + 98m_W^2)B_0(0,m_W^2,m_W^2) + (402m_W^2 - 33m_H^2) \\
 & \times B_0(m_H^2,m_W^2,m_W^2) + 27m_H^4C_0(m_H^2,m_H^2,0,m_W^2,m_W^2,m_W^2)\left.\right)g^{\rho\sigma} \\
 & - \left((3456D_0(m_H^2,m_H^2,0,0,0,0,m_W^2,m_W^2,m_W^2,m_W^2)m_W^6\right. \\
 & - 576m_H^2D_0(m_H^2,m_H^2,0,0,0,0,m_W^2,m_W^2,m_W^2,m_W^2)m_W^4 + 900m_W^2 + 86m_H^2 \\
 & - 144(5m_H^2m_W^2 - 12m_W^4)C_0(m_H^2,0,0,m_W^2,m_W^2,m_W^2) \\
 & + 9(m_H^4 + 6m_W^2m_H^2 + 104m_W^4)C_0(m_H^2,m_H^2,0,m_W^2,m_W^2,m_W^2)m_H^2 \\
 & + (-9m_H^4 - 474m_W^2m_H^2 + 864m_W^4)B_0(0,m_W^2,m_W^2) \\
 & \left.\left.+ (-51m_H^4 + 474m_W^2m_H^2 - 864m_W^4)B_0(m_H^2,m_W^2,m_W^2)\right)k^\rho p^\sigma\right)\varepsilon^{*\rho}(p)\varepsilon^{*\sigma}(k)
 \end{aligned} \tag{5.34}$$

$$\begin{aligned}
 i\mathcal{F}_{O_{WW}}^{EffProp(b)} = & -\frac{ie^2g}{288m_H^4m_W\pi^2}f_{WW}\left(m_H^4\left(864D_0(m_H^2,0,0,0,0,0,m_W^2,m_W^2,m_W^2,m_W^2)m_W^8\right.\right. \\
 & + 864C_0(m_H^2,0,0,m_W^2,m_W^2,m_W^2)m_W^6 \\
 & - 144m_H^2D_0(m_H^2,0,0,0,0,0,m_W^2,m_W^2,m_W^2,m_W^2)m_W^6 \\
 & - 288m_H^2C_0(m_H^2,0,0,m_W^2,m_W^2,m_W^2)m_W^4 + 297m_W^4 + 14m_H^2m_W^2 - 2m_H^4 \\
 & - 6(5m_H^2m_W^2 - 47m_W^4)B_0(0,m_W^2,m_W^2) + 3(5m_H^4 - 34m_W^2m_H^2 + 32m_W^4) \\
 & \times B_0(m_H^2,m_W^2,m_W^2)\left.\right)g^{\rho\sigma} - 2\left((-216(m_H^2 - 2m_W^2)\right. \\
 & \times D_0(m_H^2,0,0,0,0,0,m_W^2,m_W^2,m_W^2,m_W^2)m_W^6 \\
 & - 288(m_H^2 - 3m_W^2)C_0(m_H^2,0,0,m_W^2,m_W^2,m_W^2)m_W^4 + 216m_W^4m_H^2 \\
 & + 34m_H^2m_W^2 - m_H^4) - 6m_W^2(m_H^4 - 22m_W^2m_H^2 + 144m_W^4)B_0(0,m_W^2,m_W^2) \\
 & \left.\left.+ 3(m_H^6 - 8m_W^2m_H^4 - 44m_W^4m_H^2 + 288m_W^6)B_0(m_H^2,m_W^2,m_W^2)\right)k^\rho p^\sigma\right) \\
 & \times \varepsilon^{*\rho}(p)\varepsilon^{*\sigma}(k)
 \end{aligned} \tag{5.35}$$

$$\begin{aligned}
 i\mathcal{F}_{O_{WW}}^{EffProp(d)} &= \frac{ie^2 g m_W}{576 m_H^2 \pi^2} f_{WW} \left(\left(27C_0(m_H^2, m_H^2, 0, m_W^2, m_W^2, m_W^2) m_H^4 \right. \right. \\
 &\quad - 126m_W^2 C_0(m_H^2, m_H^2, 0, m_W^2, m_W^2, m_W^2) m_H^2 + 14m_H^2 + 36m_W^2 \\
 &\quad - 3(9m_H^2 + 2m_W^2) B_0(0, m_W^2, m_W^2) + (330m_W^2 - 69m_H^2) B_0(m_H^2, m_W^2, m_W^2) \\
 &\quad \left. \left. + 360m_W^4 C_0(m_H^2, m_H^2, 0, m_W^2, m_W^2, m_W^2) \right) g^{\rho\sigma} m_H^2 \right. \\
 &\quad + \left(-9C_0(m_H^2, m_H^2, 0, m_W^2, m_W^2, m_W^2) m_H^4 + 90m_W^2 C_0(m_H^2, m_H^2, 0, m_W^2, m_W^2, m_W^2) m_H^2 \right. \\
 &\quad - 14m_H^2 - 36m_W^2 + (9m_H^2 + 42m_W^2) B_0(0, m_W^2, m_W^2) (51m_H^2 - 42m_W^2) \\
 &\quad \left. \left. \times B_0(m_H^2, m_W^2, m_W^2) - 72m_W^4 C_0(m_H^2, m_H^2, 0, m_W^2, m_W^2, m_W^2) \right) k^\rho p^\sigma \right) \\
 &\quad \times \varepsilon^{*\rho}(p) \varepsilon^{*\sigma}(k). \tag{5.36}
 \end{aligned}$$

Loops (c) and (e) give apparently the same results as (a) and (d), respectively, since there is an obvious symmetry.

Summing it all together, we get the final result for operator O_{WW} :

$$\begin{aligned}
 i\mathcal{F}_{O_{WW}} &= -\frac{ie^2 g}{128 m_H^2 m_W \pi^2} f_{WW} \left(3B_0(m_H^2, m_H^2, m_H^2) m_H^4 \right. \\
 &\quad + 32 \left((24D_0(m_H^2, m_H^2, 0, 0, 0, 0, m_W^2, m_W^2, m_W^2, m_W^2) m_H^4 \right. \\
 &\quad - 2(m_H^2 - 6m_W^2) D_0(m_H^2, 0, 0, 0, 0, 0, m_W^2, m_W^2, m_W^2, m_W^2) m_W^2 \\
 &\quad - 4m_H^2 D_0(m_H^2, m_H^2, 0, 0, 0, 0, m_W^2, m_W^2, m_W^2, m_W^2) \\
 &\quad \left. \left. + m_W^2 + (m_H^2 + 6m_W^2) C_0(m_H^2, m_H^2, 0, m_W^2, m_W^2, m_W^2) + 6 \right) m_W^4 \right. \\
 &\quad \left. \left. + (m_H^4 - 7m_W^2 m_H^2 + 18m_W^4) C_0(m_H^2, 0, 0, m_W^2, m_W^2, m_W^2) m_W^2 \right) \right) \\
 &\quad \times (m_H^2 g^{\rho\sigma} - 2k^\rho p^\sigma) \varepsilon^{*\rho}(p) \varepsilon^{*\sigma}(k) \tag{5.37}
 \end{aligned}$$

One interesting fact is worth mentioning here - when we look at the partial results (5.29) through (5.36) we find that unlike in the case of previous operator O_{WWW} , none of the individual results is transverse with respect to the external photon momenta. Only when we sum everything together, we achieve full transversality, and in the final result we can pull out transverse factor $(m_H^2 g^{\rho\sigma} - 2k^\rho p^\sigma)$ - see (5.37).

5.2.3 Contribution of the operator O_W

Affected interactions will be: $W^+W^-\gamma$, W^+W^-H and $HW^+W^-\gamma$. This will apparently contribute to SM-like graphs (a), (b), (d) and (e) - Fig. 5.9, and new topology graph (b) - Fig. 5.2. Corresponding Feynman rules will be:

$$V_{O_W}^{WW\gamma} = \frac{1}{2} i e f_W m_W^2 (g^{\lambda\nu} k^\mu - g^{\lambda\mu} k^\nu) \quad (5.38)$$

$$V_{O_W}^{WWH} = -\frac{1}{2} i g f_W m_W (q^\mu h^\nu + h^\mu p^\nu - g^{\mu\nu} (h \cdot p + h \cdot q)) \quad (5.39)$$

$$V_{O_W}^{WWH\gamma} = -\frac{1}{2} i e g f_W m_W (g^{\lambda\nu} (h^\mu - k^\mu) + g^{\lambda\mu} (k^\nu - h^\nu)). \quad (5.40)$$

Again, the vertex and impulse notation is the same as in previous section and will stay that way unless said otherwise. The way of constructing effective loops is straightforward and similar to previous cases, so we will present just the Feynman rules and final results for each effective operator from now on. When summed together, graphs originating from the operator O_W will give the final result:

$$\begin{aligned} i\mathcal{F}_{O_W} &= \frac{i e^2 g}{64 m_W \pi^2} f_W \left[(m_H^2 - 2m_W^2) \left(8 C_0(m_H^2, 0, 0, m_W^2, m_W^2, m_W^2) m_W^2 \right. \right. \\ &\quad \left. \left. + B_0(m_H^2, m_W^2, m_W^2) \right) - 4 m_W^2 B_0(0, m_W^2, m_W^2) \right] \\ &\quad \times (m_H^2 g^{\rho\sigma} - 2k^\rho p^\sigma). \end{aligned} \quad (5.41)$$

Again, transversality of the result can be confirmed by pinpointing the transverse factor

$$(m_H^2 g^{\rho\sigma} - 2k^\rho p^\sigma). \quad (5.42)$$

5.2.4 Contribution of the operator O_{DW}

Affected interactions will be: $W^+W^-\gamma$, $W^+W^-\gamma\gamma$ and W^+W^- (propagator). So, besides the SM-like graphs (a), (b) and (c) on Fig. 5.9, we are also going to get all the graphs from Fig. 5.8. Feynman rules for O_{DW} operator are:

$$\begin{aligned} V_{O_{DW}}^{WW\gamma} &= -2 i e g^2 f_{DW} \left[g^{\lambda\mu} \left(p^\nu (2k \cdot p + p \cdot q) - k^\nu (2k \cdot p + k \cdot q) \right) \right. \\ &\quad \left. + g^{\lambda\nu} \left(k^\mu (k \cdot p + 2k \cdot q) - q^\mu (2k \cdot q + p \cdot q) \right) \right. \\ &\quad \left. + p^\lambda \left(k^\mu (k^\nu - p^\nu) + q^\mu p^\nu - g^{\mu\nu} (k \cdot p + 2p \cdot q) \right) \right] \end{aligned}$$

$$+ q^\lambda \left(-k^\mu k^\nu + q^\mu (k^\nu - p^\nu) + g^{\mu\nu} (k \cdot q + 2p \cdot q) \right) \Big] \quad (5.43)$$

$$\begin{aligned} V_{ODW}^{WW\gamma\gamma} = & 2i e^2 g^2 f_{DW} \left[(p^\lambda (k^\mu - q^\mu) + q^\lambda q^\mu + r^\lambda (-k^\mu - 2q^\mu + r^\mu)) g^{\nu\rho} \right. \\ & - g^{\lambda\mu} (2k \cdot p + k \cdot r + p \cdot q + 2q \cdot r) g^{\nu\rho} + g^{\mu\rho} (q^\lambda (k^\nu - p^\nu) + p^\lambda p^\nu + r^\lambda (-k^\nu - 2p^\nu + r^\nu)) \\ & + g^{\lambda\rho} (r^\mu (2k^\nu + p^\nu - 2r^\nu) + q^\mu (k^\nu - 2p^\nu + r^\nu) + k^\mu (-2k^\nu + p^\nu + 2r^\nu)) \\ & + g^{\lambda\mu} (k^\nu k^\rho + p^\nu (-2k^\rho + p^\rho - q^\rho) + r^\nu (q^\rho - k^\rho)) + g^{\lambda\nu} (k^\mu k^\rho + r^\mu (p^\rho - k^\rho) \\ & + q^\mu (-2k^\rho - p^\rho + q^\rho)) + g^{\mu\nu} (q^\lambda (k^\rho + 2p^\rho - 2q^\rho) + r^\lambda (-2k^\rho + p^\rho + q^\rho) \\ & + p^\lambda (k^\rho - 2p^\rho + 2q^\rho)) - g^{\lambda\nu} g^{\mu\rho} (2k \cdot q + k \cdot r + p \cdot q + 2p \cdot r) \\ & \left. + g^{\lambda\rho} g^{\mu\nu} (k \cdot p + k \cdot q + 4k \cdot r + 4p \cdot q + p \cdot r + q \cdot r) \right] \quad (5.44) \end{aligned}$$

$$V_{ODW}^{WW} = 2i g^2 p^2 f_{DW} (p^\lambda p^\mu - g^{\lambda\mu} p^2), \quad (5.45)$$

and the final result for O_{DW} will be:

$$\begin{aligned} i\mathcal{F}_{ODW} = & -\frac{ie^2 g^3}{8m_H^2 \pi^2} m_W f_{DW} \left[-6B_0(0, m_W^2, m_W^2) m_H^2 - 12B_0(m_H^2, m_W^2, m_W^2) m_H^2 + 7m_H^2 \right. \\ & + 12m_W^2 + 2m_W^2 \left(2(6m_W^2 - m_H^2) (D_0(m_H^2, 0, 0, 0, 0, 0, m_W^2, m_W^2, m_W^2, m_W^2)) \right. \\ & \left. + 2D_0(m_H^2, m_H^2, 0, 0, 0, 0, m_W^2, m_W^2, m_W^2, m_W^2) \right) m_W^2 - 6(2m_H^2 - 3m_W^2) \\ & \times C_0(m_H^2, 0, 0, m_W^2, m_W^2, m_W^2) + (m_H^2 + 6m_W^2) \\ & \left. \left. \times C_0(m_H^2, m_H^2, 0, m_W^2, m_W^2, m_W^2) \right) \right] (m_H^2 g^{\rho\sigma} - 2k^\rho p^\sigma). \quad (5.46) \end{aligned}$$

5.2.5 Contribution of the operator O_{BW}

We get the following Feynman rules and interactions here:

$$V_{OBW}^{WW\gamma} = -ie m_W^2 f_{BW} (g^{\lambda\nu} k^\mu - g^{\lambda\mu} k^\nu) \quad (5.47)$$

$$V_{OBW}^{HWW\gamma} = ie g m_W f_{BW} (g^{\lambda\mu} k^\nu - g^{\lambda\nu} k^\mu) \quad (5.48)$$

$$V_{OBW}^{HH\gamma\gamma} = ie^2 f_{BW} (r^\lambda k^\rho - g^{\lambda\rho} k \cdot r), \quad (5.49)$$

and the result will be:

$$\begin{aligned}
 i\mathcal{F}_{O_{BW}} &= \frac{ie^2g}{128m_W\pi^2} \left(32C_0(m_H^2, 0, 0, m_W^2, m_W^2, m_W^2) m_W^4 + 16B_0(0, m_W^2, m_W^2) m_W^2 \right. \\
 &\quad + 8B_0(m_H^2, m_W^2, m_W^2) m_W^2 - 16m_W^2 + 3m_H^2 B_0(m_H^2, m_H^2, m_H^2) \\
 &\quad \left. - 4m_H^2 B_0(m_H^2, m_W^2, m_W^2) \right) (m_H^2 g^{\rho\sigma} - 2k^\rho p^\sigma). \quad (5.50)
 \end{aligned}$$

5.2.6 Contribution of the operator O_{BB}

In case of this operator, we get only one interaction

$$V_{O_{BB}}^{HH\gamma\gamma} = ie^2 f_{BB} (g^{\lambda\rho} k \cdot r - r^\lambda k^\rho) \quad (5.51)$$

which gives the following result:

$$i\mathcal{F}_{O_{BB}} = -\frac{3ie^2 g f_{BB} m_H^2 B_0(m_H^2, m_H^2, m_H^2) (m_H^2 g^{\rho\sigma} - 2k^\rho p^\sigma)}{128m_W\pi^2}. \quad (5.52)$$

5.2.7 Contribution of the operator O_B

We get the following Feynman rules and interactions here:

$$V_{O_B}^{WW\gamma} = \frac{1}{2} ie m_W^2 f_B (g^{\lambda\nu} k^\mu - g^{\lambda\mu} k^\nu) \quad (5.53)$$

$$V_{O_B}^{HWW\gamma} = \frac{1}{2} ie g m_W f_B (g^{\lambda\nu} k^\mu - g^{\lambda\mu} k^\nu) \quad (5.54)$$

and the result is:

$$\begin{aligned}
 i\mathcal{F}_{O_{BB}} &= -\frac{ie^2g}{64m_W\pi^2} f_B \left(8C_0(m_H^2, 0, 0, m_W^2, m_W^2, m_W^2) m_W^4 + 4B_0(0, m_W^2, m_W^2) m_W^2 \right. \\
 &\quad \left. - 4m_W^2 - (m_H^2 - 2m_W^2) B_0(m_H^2, m_W^2, m_W^2) \right) (m_H^2 g^{\rho\sigma} - 2k^\rho p^\sigma). \quad (5.55)
 \end{aligned}$$

5.2.8 Contribution of operators $O_{DB}, O_{\Phi,1}, O_{\Phi,2}$ and $O_{\Phi,3}$

These operators due to their field structure do not contribute to $H \rightarrow \gamma\gamma$ process.

5.2.9 Overall contribution of dimension-six operators to $H \rightarrow \gamma\gamma$ process at one-loop level

When we sum together all the partial results for individual operators, we get the final result for the matrix element of $H \rightarrow \gamma\gamma$ process at one-loop level:

$$\begin{aligned}
 i M_{\text{eff}}^{\text{loop}}(H \rightarrow \gamma\gamma) = & -\frac{i e^2 g}{128 m_W \pi^2} \left\{ 8 \left[f_B^\Lambda - 2f_{BW}^\Lambda + f_W^\Lambda + 3g^2(-4f_{DW}^\Lambda + f_{WWW}^\Lambda) \right] m_H^2 m_W^2 B_0(0, m_W^2, m_W^2) \right. \\
 & - 3(f_{BB}^\Lambda - f_{BW}^\Lambda + f_{WW}^\Lambda) m_H^4 B_0(m_H^2, m_H^2, m_H^2) \\
 & + 2 \left[m_H^2 \left((f_B^\Lambda - 2f_{BW}^\Lambda + f_W^\Lambda) m_H^2 - 2(f_B^\Lambda - 2f_{BW}^\Lambda + f_W^\Lambda \right. \right. \\
 & \left. \left. + 12g^2(-4f_{DW}^\Lambda + f_{WWW}^\Lambda)) m_W^2 \right) B_0(m_H^2, m_W^2, m_W^2) \right. \\
 & \left. + 4m_W^2 \left[\left(f_B^\Lambda - 2(f_{BW}^\Lambda + 7g^2 f_{DW}^\Lambda) + 3g^2 f_{WWW}^\Lambda \right) m_H^2 - 24(g^2 f_{DW}^\Lambda + f_{WW}^\Lambda) m_W^2 \right. \right. \\
 & \left. \left. + 2 \left((f_W^\Lambda - 2f_{WW}^\Lambda) m_H^4 - (f_B^\Lambda - 2f_{BW}^\Lambda + 2(f_W^\Lambda - 7f_{WW}^\Lambda) \right. \right. \right. \\
 & \left. \left. + 3g^2(-8f_{DW}^\Lambda + f_{WWW}^\Lambda)) m_H^2 m_W^2 - 36(g^2 f_{DW}^\Lambda + f_{WW}^\Lambda) m_W^4 \right) \right. \\
 & \left. \times C_0(m_H^2, 0, 0; m_W^2, m_W^2, m_W^2) \right. \\
 & \left. + 4(g^2 f_{DW}^\Lambda + f_{WW}^\Lambda) m_W^2 \left(-(m_H^2 + 6m_W^2) C_0(m_H^2, m_H^2, 0; m_W^2, m_W^2, m_W^2) \right. \right. \\
 & \left. \left. - 2m_W^2(-m_H^2 + 6m_W^2)(D_0(m_H^2; m_W^2) + 2D_0(m_H^2, m_H^2; m_W^2)) \right) \right] \left. \right\} \\
 & \times \left(g^{\rho\sigma} - \frac{2k^\rho p^\sigma}{m_H^2} \right) \varepsilon_\mu^*(p) \varepsilon_\nu^*(k), \tag{5.56}
 \end{aligned}$$

where we denote

$$\begin{aligned}
 D_0(m_H^2; m_W^2) & \equiv D_0(m_H^2, 0, 0, 0, 0, 0; m_W^2, m_W^2, m_W^2, m_W^2) \\
 D_0(m_H^2, m_H^2; m_W^2) & \equiv D_0(m_H^2, m_H^2, 0, 0, 0, 0; m_W^2, m_W^2, m_W^2, m_W^2)
 \end{aligned}$$

and $f_i^\Lambda = f_i/\Lambda^2$.

The result (5.56) apparently contains a lot of free parameters in the form of the effective coupling constants f_i . We will discuss these matters in the next chapter.

Chapter 6

Renormalization

6.1 Renormalization in quantum field theories

In this section we are going to give a brief systematic review of a subject of renormalization in quantum field theories. More detailed discussion of the subject can be found in [11]. When performing loop momentum integrations of Feynman diagrams in higher orders of perturbation theory (i.e. the diagrams with at least one loop), we may encounter problems that integrals become divergent for small and high values of momentum. Such divergences are called *infrared* and *ultra-violet divergences* respectively. We do not encounter infrared divergences in our calculations, so we will not address this issue here and further concentrate only on the area of ultraviolet (UV) divergences. UV divergences turned out to be a quite common feature of quantum field theories. Typical and well known UV divergent diagrams of QED are shown in figure 6.1.

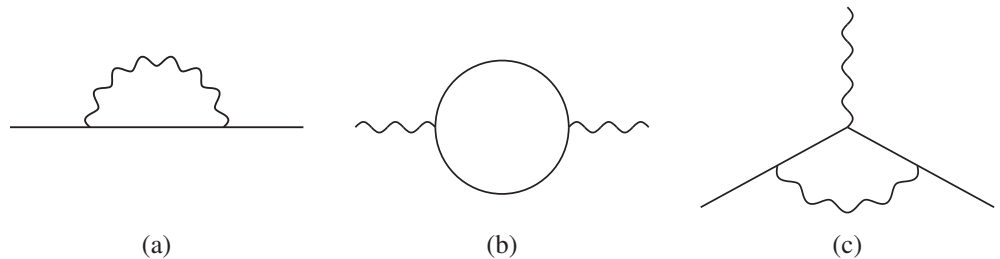


Figure 6.1: Three well known divergent one-loop diagrams of QED

When we look at the diagram (b), it has the following structure:

$$-i\Pi_{\mu\nu}(q) = (-1) \int \frac{d^4l}{(2\pi)^4} \text{Tr} \left(\gamma_\mu \frac{1}{\not{l} - \not{q} - m} \gamma_\nu \frac{1}{\not{l} - m} \right) \quad (6.1)$$

and its UV divergence is obvious. We will use *QED* and *scalar field theory* to point out all peculiarities of renormalization because they have simple structure, cover all crucial features, and can easily be generalized to any quantum field theory. More general QED loop diagram can look something like this:

$$\int \frac{d^4k_1 d^4k_2 \dots d^4k_L}{(k_i - m) \dots (k_j^2) \dots (k_n^2)}. \quad (6.2)$$

For each loop there is a potentially divergent 4-momentum integral, but each propagator helps the convergence of such integral by putting one or two powers of the momentum into the denominator. Roughly speaking, the diagram diverges if there are more powers of momentum in the numerator, when the power of momentum is higher for the denominator, it converges. We can therefore define the *superficial degree of divergence* D as follows:

$$\begin{aligned} D &\equiv \text{power of } k \text{ in the numerator} - \text{power of } k \text{ in the denominator} \\ &= 4L - P_e - 2P_\gamma, \end{aligned} \quad (6.3)$$

where P_e stands for the number of electron propagators and P_γ for the number of photon propagators. Let us consider a parameter Λ^D where Λ is a momentum cutoff. Naively, one could expect a diagram to be divergent for $D > 0$, and for $D = 0$, a divergence proportional to the $\log \Lambda$. For $D < 0$, one could expect no divergence. Such “naive” expectation can be and is often wrong for various reasons. If a diagram contains a divergent sub-diagram, its divergence can be higher than the one indicated by D . On the other hand, if some symmetries (such as the Ward identity) cause some terms to cancel, the divergence may be lower than indicated by D , or it may even vanish completely. Despite these facts, D is still a very useful quantity. To get further information, number of loop integrations L can be rewritten as

$$L = P_e + P_\gamma - V + 1, \quad (6.4)$$

where V stands for the overall number of vertices. Formula (6.4) can be easily assembled if we realize that each propagator adds one momentum integral, each vertex has a delta function, and one delta function assures overall momentum conservation. We can subsequently rewrite the number of vertices as

$$V = 2P_\gamma + N_\gamma = \frac{1}{2}(2P_e + N_e) \quad (6.5)$$

with N_γ representing the number of external photon lines and N_e the number of external electron lines. (6.5) represents the fact that each vertex consists of just one photon line and two electron lines. The propagators we have to count twice since they have two ends, each connected to one vertex. Putting it all together, we can express D as

$$D = 4 - N_\gamma - \frac{3}{2}N_e. \quad (6.6)$$

The good aspect of formula (6.6) is the fact that the superficial degree of divergence of QED diagram does not depend on the number of vertices, and depends only on the number of external legs of each type. Such property of a theory is very desirable because it means that only a finite number of *amplitudes* will be divergent. We will return to this issue later.

In order to be able to see some more general aspects of the problem, we will now generalize QED into d dimensions. We will soon discover that in four dimensions it has by coincidence some rather special properties. In this case D is given by

$$D \equiv dL - P_e - 2P_\gamma, \quad (6.7)$$

since each loop generates a d -dimensional momentum integral. The validity of relations (6.4) and (6.5) is not impaired even here, so we can write:

$$D = d + \left(\frac{d-4}{2}\right) V - \left(\frac{d-2}{2}\right) N_\gamma - \left(\frac{d-1}{2}\right) N_e. \quad (6.8)$$

We can now see clearly that the cancellation of term containing V in (6.6) was really a coincidence in case of $d = 4$. For the case of $d < 4$, diagrams with more vertices have a lower degree of divergence which means only a *finite number of diagrams* is divergent. On the other hand, for the case of $d > 4$, diagrams with more vertices have a higher degree of divergence which means that *every amplitude* will sooner or later become divergent at sufficiently high order of perturbation theory. Such three types of behavior in the ultraviolet area can be generalized to all quantum field theories. We can therefore divide them into three distinctive groups:

- Super-Renormalizable theory: Only a finite number of Feynman diagrams superficially diverge.
- Renormalizable theory: Only a finite number of amplitudes superficially diverge, however, divergences appear at all orders in perturbation theory.
- Non-Renormalizable theory: All amplitudes are divergent at sufficiently high order of perturbation theory.

The reason for using such names will become apparent once we establish a procedure of eliminating the divergent parts of the diagrams. Using this terminology, we can say that QED is renormalizable in four dimensions, super-renormalizable in less than four dimensions and non-renormalizable in more than four dimensions. These criteria give a correct picture of a true divergence of the theory in most cases, as we have mentioned above. Let us now look at another simple quantum field theory - a scalar field theory in d dimensions:

$$\mathcal{L} = \frac{1}{2}(\partial_\mu\phi)^2 - \frac{1}{2}m^2\phi^2 - \frac{\lambda}{n!}\phi^n. \quad (6.9)$$

The overall number of loops in a diagram is similar as in (6.4):

$$L = P - V + 1, \quad (6.10)$$

where P now stands for the number of scalar propagators. For n lines meeting at each vertex with N representing the number of external lines, we can write $nV = N + 2P$. We can easily write formula for a superficial degree of divergence of a scalar theory diagram:

$$D = dL - 2P \quad (6.11)$$

$$= d + \left[n \left(\frac{d-2}{2} \right) - d \right] V - \left(\frac{d-2}{2} \right) N. \quad (6.12)$$

In four dimensions, ϕ^4 coupling is renormalizable while higher powers of ϕ are not. When we go to three dimensions, ϕ^6 becomes renormalizable while ϕ^4 is even super-renormalizable.

Formulas (6.8) and (6.12) can be also looked at from a somewhat different angle: the dimensionality of coupling constants. In all quantum field theories, since we work in units where $\hbar = 1$, the action $S = \int d^d x \mathcal{L}$ must be dimensionless. In such unit system, the integral $d^d x$ has the dimension of $(\text{mass})^{-d}$, therefore the Lagrangian must have dimension of $(\text{mass})^d$. Using this fact, we can infer the dimension of the scalar field from the kinetic term of (6.9) - ϕ has dimension $(d-2)/2$. From the interaction term in (6.9) and the dimension of ϕ , we can deduce that λ has the dimension of $d - n(d-2)/2$. But if we look at (6.12), we see that it is just the factor that multiplies V with the opposite sign. We arrive at the same correspondence for coupling constant if we look at the equation (6.8) for the QED, and any other quantum field theory whatsoever. More rigorous proof of this can be found at [11]. Looking again at (6.12), we see that for coupling constant with *positive mass dimension* D will be decreasing with growing number of vertices in a diagram, and therefore only a limited number of diagrams will diverge and so on. Thus, we can divide all quantum field theories into the same three categories, based on the second criteria - the dimension of the coupling constant:

Super-Renormalizable theory:	Coupling constant has a positive dimension of mass.
Renormalizable theory:	Coupling constant is dimensionless.
Non-Renormalizable theory:	Coupling constant has a negative dimension of mass.

QED has a dimensionless coupling constant, therefore by this criteria it is superficially renormalizable.

The first reaction to the appearance of divergences is that any theory containing such divergences must be somehow wrong. But this attitude is somewhat restrictive, as it excludes pretty much all quantum field theories, because as we have

stated already, the presence of the divergences is quite common. It is therefore desirable to develop more tolerant attitude towards them. We can assume such approach, that we can live with these divergences as long as they do not appear in physical predictions. Such goal can be accomplished by absorbing the infinite parts of the diagrams into the redefinition of theory's parameters, such as coupling constants and masses. This can be done systematically for every quantum field theory through the introduction of *counterterms* - the parts of Lagrangian that will have such structure, that it will cancel the divergent parts of diagrams. Subtracting infinite expressions of course does not make sense, so we have to first find some way to render the expressions finite, depending on some parameter with the expressions growing infinite only in certain limit of that parameter. Such procedure is called *regularization*. We then cancel the potentially infinite terms with the aid of counterterms, and finally perform the limit which will now give finite expression. If the counterterms we require have the same structure as the terms that are already present in the original Lagrangian of our theory, we do not need to add those counterterms "by hand", but we simply state that the parameters contained (usually called *bare values*) in the original Lagrangian aren't those we measure, but rather some unphysical values. Subsequently, we split those bare values into the physical part and to the counterterm part that will later cancel some divergent part of the diagram. In such manner, we can perform what is refer to as renormalization of theory's parameters and wave functions. However, sometimes counterterms with different structure than those contained in the original Lagrangian are also required, in such case we need to add them "by hand". We will see such example in the next paragraph. Looking back at the Lagrangian (6.9) we now write

$$\mathcal{L} = \frac{1}{2}(\partial_\mu\phi)^2 - \frac{1}{2}m_0^2\phi^2 - \frac{\lambda_0}{n!}\phi^n \quad (6.13)$$

with m_0 and λ_0 representing now the bare unphysical values. The bare values will be split

$$m_0^2 = \delta_m + m^2 \quad \lambda_0 = \delta_\lambda + \lambda \quad (6.14)$$

with λ and m being the physical values and δ_m and δ_λ the counterterm parts. Lagrangian (6.13) then becomes:

$$\begin{aligned} \mathcal{L} &= \frac{1}{2}(\partial_\mu\phi)^2 - \frac{1}{2}m^2\phi^2 - \frac{\lambda}{n!}\phi^n \\ &\quad - \frac{1}{2}\delta_m\phi^2 - \frac{\delta_\lambda}{n!}\phi^n. \end{aligned} \quad (6.15)$$

One of the divergent diagrams of the scalar field theory is shown on the figure 6.2 and in (6.16):

$$I = \frac{(-i\lambda)^2}{2} \int \frac{d^4l}{(2\pi)^4} \frac{i}{l^2 - m^2} \frac{i}{(l+p)^2 - m^2}. \quad (6.16)$$

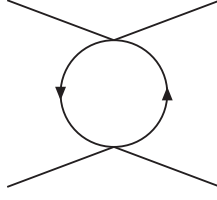


Figure 6.2: One divergent graph of the scalar field theory

(6.16) can be easily evaluated by the means of Passarino-Veltman reduction:

$$I = \frac{1}{2}i\pi^2\lambda^2 B_0(p^2, m^2, m^2). \quad (6.17)$$

Taking all possible diagrams of this amplitude at one loop level into account (which are related to each other by crossing symmetry), p^2 is equal to Mandelstam variables s, t and u .

Now would be a good time to give just a brief summary of the *regularization* procedure. We are going to employ a method known as *dimensional regularization* in which we render the integral convergent by generalizing it into n dimensions. Divergence then exists as a limit for $n \rightarrow 4$. There are also other methods, such us *Pauli-Villars regularization*, which we will not discuss here. Full fledged derivation is given in [11].

Let us look again on the expression (6.1). First, we are going to generalize it into n dimensions:

$$-i\Pi_{\mu\nu}^{DR}(q) = (-1) \int \frac{d^n l}{(2\pi)^n} \text{Tr} \left(\gamma_\mu \frac{1}{\not{l} + \not{q} - m} \gamma_\nu \frac{1}{\not{l} - m} \right) \cdot \mu^{4-n}, \quad (6.18)$$

where we have added arbitrary mass parameter μ in order to keep the dimensionality right. By m^2 we in fact mean $m^2 - i\epsilon$. After a simple manipulation, we get:

$$\begin{aligned} i\Pi_{\mu\nu}^{DR}(q) &= \int \frac{d^n l}{(2\pi)^n} \text{Tr} [\gamma_\mu (\not{l} + m) \gamma_\nu (\not{l} + \not{q} + m)] \\ &\quad \times \frac{1}{[(l+q)^2 - m^2][l^2 - m^2]}. \end{aligned} \quad (6.19)$$

Introducing the Feynman parameterization

$$\frac{1}{ab} = \int_0^1 dx \frac{1}{[ax + b(1-x)]^2} = \int_0^1 dx \frac{1}{[(a-b)x + b]^2} \quad (6.20)$$

and some simple manipulations, we get:

$$i\Pi_{\mu\nu}^{DR}(q) = \int_0^1 dx \int \frac{d^n l}{(2\pi)^n} Tr[\dots] \frac{1}{[(l+xq)^2 - x^2 q^2 + xq^2 - m^2]^2}. \quad (6.21)$$

After performing integration variable shift $l+xq=l'$ and discarding terms proportional to odd powers of l due to symmetry, we arrive at:

$$\begin{aligned} \frac{1}{4}i\Pi_{\mu\nu}^{DR}(q) &= \int_0^1 dx \int \frac{d^n l}{(2\pi)^n} [-x(1-x)(2g_\mu g_\nu - 2q^2 g_{\mu\nu})] \cdot \frac{1}{(l^2 - C)^2} \\ &- g_{\mu\nu} \frac{1}{(l^2 - C)^2} [q^2 x(1-x) - (\frac{2}{n} - 1)l^2 - m^2] \end{aligned} \quad (6.22)$$

with $C = m^2 - x(1-x)q^2$. We are now going to employ formula

$$\int \frac{d^n l}{(2\pi)^n} \frac{(l^2)^r}{(l^2 - C + i\epsilon)^s} = \frac{i(-1)^{r-s}}{(4\pi)^{n/2}} C^{r+\frac{n}{2}-s} \frac{\Gamma(r+\frac{n}{2})\Gamma(s-r-\frac{n}{2})}{\Gamma(\frac{n}{2})\Gamma(s)}, \quad (6.23)$$

which can be proved with the help of *Wick rotation*. With the aid of (6.23), we can easily see that second part of (6.22) vanishes. Employing (6.23), we get

$$i\Pi_{\mu\nu}^{DR}(q) = (q^2 g_{\mu\nu} - q_\mu q_\nu) i\Pi^{DR}(q^2) \quad (6.24)$$

with

$$i\Pi_{\mu\nu}^{DR}(q^2) = \mu^{4-n} \int_0^1 dx 8x(1-x) \frac{i}{(4\pi)^{\frac{n}{2}}} C^{\frac{n}{2}-2} \frac{\Gamma(\frac{n}{2})\Gamma(2-\frac{n}{2})}{\Gamma(\frac{n}{2})\Gamma(2)}. \quad (6.25)$$

(6.25) can be easily put in the form:

$$\Pi_{\mu\nu}^{DR}(q^2) = \frac{1}{2\pi^2} (4\pi)^\varepsilon \Gamma(\varepsilon) \int_0^1 dx x(1-x) \left(\frac{C}{\mu^2}\right)^{-\varepsilon} \quad (6.26)$$

with $\varepsilon = 2 - \frac{n}{2}$ and $\Gamma(\varepsilon)$ containing the UV-divergent part for $\varepsilon \rightarrow 0$ ($n \rightarrow 4$). Utilizing the formula $\Gamma(\varepsilon) = \frac{1}{\varepsilon} - \gamma_E + O(\varepsilon)$ with $\gamma_E \doteq 0,577$ being *Euler constant* and expanding other terms in (6.26) in ε , we arrive at the final expression:

$$\Pi_{\mu\nu}^{DR}(q^2) = \frac{1}{2\pi^2} \left(\frac{1}{6} \left(\frac{1}{\varepsilon} - \gamma_E + \ln 4\pi \right) - \int_0^1 dx x(1-x) \ln \frac{C}{\mu^2} + O(\varepsilon) \right) \quad (6.27)$$

with $\frac{1}{\varepsilon}$ now containing the “pure” UV divergence for $\varepsilon \rightarrow 0$ and the rest of the expression being perfectly convergent. So we have “surgically” isolated the UV-divergence, and it is much easier to deal with it by the means of the methods described above.

Let us return to (6.17). Evaluating it according to (A.4) in Appendix A, we can isolate the divergent part (sum of s , t and u channels) as:

$$I_{div} = \frac{3}{2} i\pi^2 \lambda^2 \frac{1}{\tilde{\varepsilon}} \quad (6.28)$$

with

$$\frac{1}{\tilde{\varepsilon}} = \frac{2}{2 - n/2} - \gamma_E + \log 4\pi. \quad (6.29)$$

Looking back at (6.15), we can quickly get the interaction counterterm with the structure we need from the last term (see Fig. 6.3).

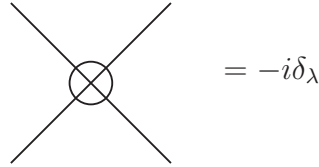
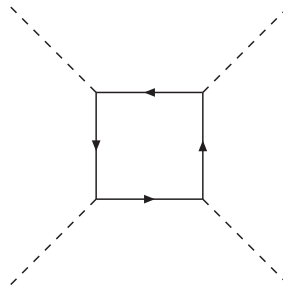


Figure 6.3: Counterterm Feynman rule for interaction term of the scalar field theory

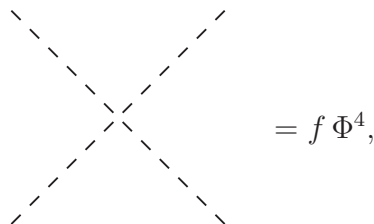
It is not true that every theory contains all its counterterms, i.e. those necessary for renormalization of all divergent diagrams that can occur within such theory. It is not even necessarily true for a theory that we classify as renormalizable: a good example of such renormalizable theory that does not contain all its counterterms would be Yukawa theory with the interaction:

$$\mathcal{L}_{Yukawa}^{int} = g \bar{\Psi} \Phi \Psi \quad (6.30)$$

with Ψ denoting fermion field and Φ scalar field. Within this theory, we can have these box-like diagrams:

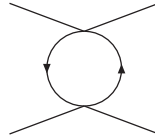


After summing all possible diagrams of this type, we get divergent result, i.e. diagrams do not cancel each other. That means we are going to require counterterm with the following structure:



which is clearly not present in the original Lagrangian and has to be added “by hand”.

Now, we are facing the final step of tuning the relations between the counterterms and their divergent counterparts in order to render the results finite. Such relations we call *renormalization conditions*. Well, the minimalist and simplest way to do it is simply posing a requirement that the counterterms cancel the divergent parts of Feynman diagrams. Such scheme is fairly simple, but has one minor disadvantage - theory’s parameters, such as coupling constants and masses, have no particular physical meaning. Nevertheless, it’s perfectly legitimate and often used for its simplicity. This scheme is usually referred to as *minimal subtraction (MS)*. There is also a slight modification where the infinite part of the counterterm is proportional to $\frac{1}{\bar{\epsilon}}$ instead of just $\frac{1}{\epsilon}$. This is usually called \overline{MS} scheme. Another possibility would be setting such requirement that λ is equal to the magnitude of the scattering amplitude at zero momentum:



$$= -i\lambda \quad \text{at } s = 4m^2, t = u = 0$$

which would represent the so-called *on shell* scheme, where the theory is renormalized in such a way that mass parameters of the theory have indeed meaning of actual masses of physical particles, propagators have accordingly poles in physical masses and other theory’s parameters have relations to physical measurable quantities. Such scheme requires the counterterms to also have finite parts, besides the infinite ones.

Working in the \overline{MS} scheme, we can finally write equation for the counterterm:

$$\delta_\lambda = -\frac{3}{2}\pi^2\lambda^2\frac{1}{\bar{\epsilon}} \quad (6.31)$$

which makes our task complete, we have eliminated divergent parts of our calculation and the result after performing a limit $n \rightarrow 4$ is finite:

$$\sum_{p^2=s,t,u} \frac{1}{2}i\pi^2\lambda^2 \left(\log \frac{m^2}{\mu^2} + 2 + \sqrt{1-4\frac{m^2}{p^2}} \log \frac{\sqrt{1-4\frac{m^2}{p^2}} - 1}{\sqrt{1-4\frac{m^2}{p^2}} + 1} \right). \quad (6.32)$$

We have shown how divergent parts of Feynman diagrams can be systematically eliminated through procedures of regularization and renormalization. Such process is always possible for super-renormalizable and renormalizable theories. We have performed renormalization procedure only to one-loop order of perturbation theory. It is obvious that it has to be performed to be consistent with whatever order of perturbation theory we do our calculations. Higher orders may bring additional

problems, such as divergent sub-diagrams and nested or overlapping divergences which have to be treated in a special way, but generally, the procedure is always performable, although the calculations can get a bit tedious sometimes.

The trouble occurs for the case of non-renormalizable theories. If we look at formulas (6.8) and (6.12), we see that for increasing number of vertices, superficial degree of divergence also rises. This means that every amplitude becomes divergent for sufficiently high order of perturbation theory. As a result, an infinite number of counterterms would be necessary for a complete renormalization of the theory. It is still possible to renormalize our calculations, since we only perform it to the finite order of perturbation theory, but it decreases the predictive power of the theory, since a lot of new free parameters is introduced. While the Standard Model fits into the above defined category of renormalizable theories, our dimension-six effective Lagrangian falls into the category of non-renormalizable theories.

6.2 Renormalization of $H \rightarrow \gamma\gamma$ at one-loop level

If we look again at the result (3.9), we see that SM result for $H \rightarrow \gamma\gamma$ contains no divergences, so what remains to be done here is the renormalization of the result (5.56) from the effective theory part. It contains a lot of B_0 scalar integrals and as we can see from Appendix A, these contain a divergent part. Divergent part of (5.56) reads as:

$$\begin{aligned}
 i M_{\text{eff}}^{\text{loop}}(H \rightarrow \gamma\gamma)_{\text{div}} &= \frac{ie^2 g (\text{mh}^2 g^{\rho\sigma} - 2k^\rho p^\sigma)}{128\pi^2 \text{mw}} \left(2f_B (\text{mh}^2 - 6\text{mw}^2) \right. \\
 &\quad - 3\text{mh}^2 f_{\text{BB}} - \text{mh}^2 f_{\text{BW}} + 24\text{mw}^2 f_{\text{BW}} \\
 &\quad + 288g^2 \text{mw}^2 f_{\text{DW}} - 72g^2 \text{mw}^2 f_{\text{WWW}} \\
 &\quad \left. + 2\text{mh}^2 f_W - 3\text{mh}^2 f_{\text{WW}} - 12\text{mw}^2 f_W \right) \frac{1}{\tilde{\epsilon}}. \quad (6.33)
 \end{aligned}$$

Counterterm with the appropriate structure will be produced by those operators that constitute the direct $H \rightarrow \gamma\gamma$ interaction, i.e. those that participate in tree-level graph of $H \rightarrow \gamma\gamma$ decay - see Fig. 6.4. Looking back to Chapter 5, section 5.1, we see that these are the operators O_{WW} , O_{BW} and O_{BB} .

Following the procedures described in previous chapter, we take the original operators as bare and divide them into the physical part and the counterterm part:

$$\begin{aligned}
 O_{\text{WW}}^0 &= O_{\text{WW}}^r + \delta O_{\text{WW}} \\
 O_{\text{BW}}^0 &= O_{\text{BW}}^r + \delta O_{\text{BW}}
 \end{aligned}$$

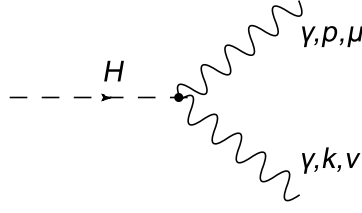


Figure 6.4: H to $\gamma\gamma$ decay at the tree level

$$O_{BB}^0 = O_{BB}^r + \delta O_{BB} \quad (6.34)$$

where superscript 0 stands for the bare operator, r for the renormalized one and prefix δ for the counterterm. The split is realized through coupling constants:

$$\begin{aligned} f_{WW}^0 &= f_{WW}^r + \delta f_{WW} \\ f_{BW}^0 &= f_{BW}^r + \delta f_{BW} \\ f_{BB}^0 &= f_{BB}^r + \delta f_{BB} \end{aligned} \quad (6.35)$$

with

$$\delta_i = \xi_i \frac{1}{\epsilon}. \quad (6.36)$$

Once we have counterterms present in these three operators, they will obviously appear in the calculation of $H \rightarrow \gamma\gamma$ at the tree level. So what we need to do, instead of just adjusting plain counterterms to compensate the divergent part of one-loop result, we will take the whole part of the tree-level result that contains counterterms and set it equal to the divergent part of one-loop result. The counterterm part of the tree-level amplitude $H \rightarrow \gamma\gamma$ (5.5) will read:

$$\frac{ie^2 m_W (\delta f_{BB} - \delta f_{BW} + \delta f_{WW}) (\text{mh}^2 g^{\rho\sigma} - 2k^\rho p^\sigma)}{g}. \quad (6.37)$$

Setting it equal to (6.33), after set of simple manipulations, we get the equation for the counterterms:

$$\begin{aligned} \xi f_{BB} - \xi f_{BW} + \xi f_{WW} &= \frac{g^2}{128\pi^2 m_W^2} \left[2f_B^r (\text{mh}^2 - 6m_W^2) - 3\text{mh}^2 f_{BB}^r \right. \\ &\quad - \text{mh}^2 f_{BW}^r + 24m_W^2 f_{BW}^r + 288g^2 m_W^2 f_{DW}^r \\ &\quad - 72g^2 m_W^2 f_{WWW}^r + 2\text{mh}^2 f_W^r - 3\text{mh}^2 f_{WW}^r \\ &\quad \left. - 12m_W^2 f_W^r \right]. \end{aligned} \quad (6.38)$$

It is obvious, that our counterterms are not uniquely determined, since we only have one equation.

So far, we have only removed the divergent parts of our calculations. It remains to be discussed what other renormalization scheme we could employ here. The vertex corrections descending from one-loop irreducible graphs here are to be taken as corrections to coupling constants which appear in tree level graphs of $H \rightarrow \gamma\gamma$ process. These are the coupling constants f_{BB} , f_{BW} and f_{WW} of the effective theory. Since these are the free parameters of the effective theory, they would need to be fixed by some experiment. Well, we don't have any such experiment at hand and therefore it is meaningless to employ any other renormalization scheme besides subtracting the divergent parts.

When we have a look at our results and formulas (A.5) and (A.6), we see that our results contain terms $\log \frac{m^2}{\mu^2}$, where m represents masses: m_H, m_W or m_Z . μ is essentially free parameter that is introduced due to regularization. Our renormalization scheme depends on such parameter. Here, and within all our calculations in this thesis, we set $\mu = m_W$ which represents a reasonable choice since it makes terms $\log \frac{m^2}{\mu^2}$ insignificantly small.

Chapter 7

Reducible graphs

Besides the one-loop irreducible graphs we have calculated in previous chapter, our theory allows us to calculate various one-loop reducible graphs. They are all depicted on Fig. 7.1. Let us apply the *on-shell* renormalization scheme here. We will now see that one of its obvious advantages is that all graphs with loop corrections on the external lines will yield zero. In our case it will be graphs (a) through (h) and (l) through (n).

7.1 One-loop corrections to the external Higgs line

Let us sum all possible one-loop corrections to the free Higgs line (these one-loop corrections are commonly known as Higgs self-energy). They correspond to graphs (a) through (f) and (l) through (n):

$$\Sigma(p^2) =$$

(a) (b,c) (d)
 (e,f) (g) (h,i)

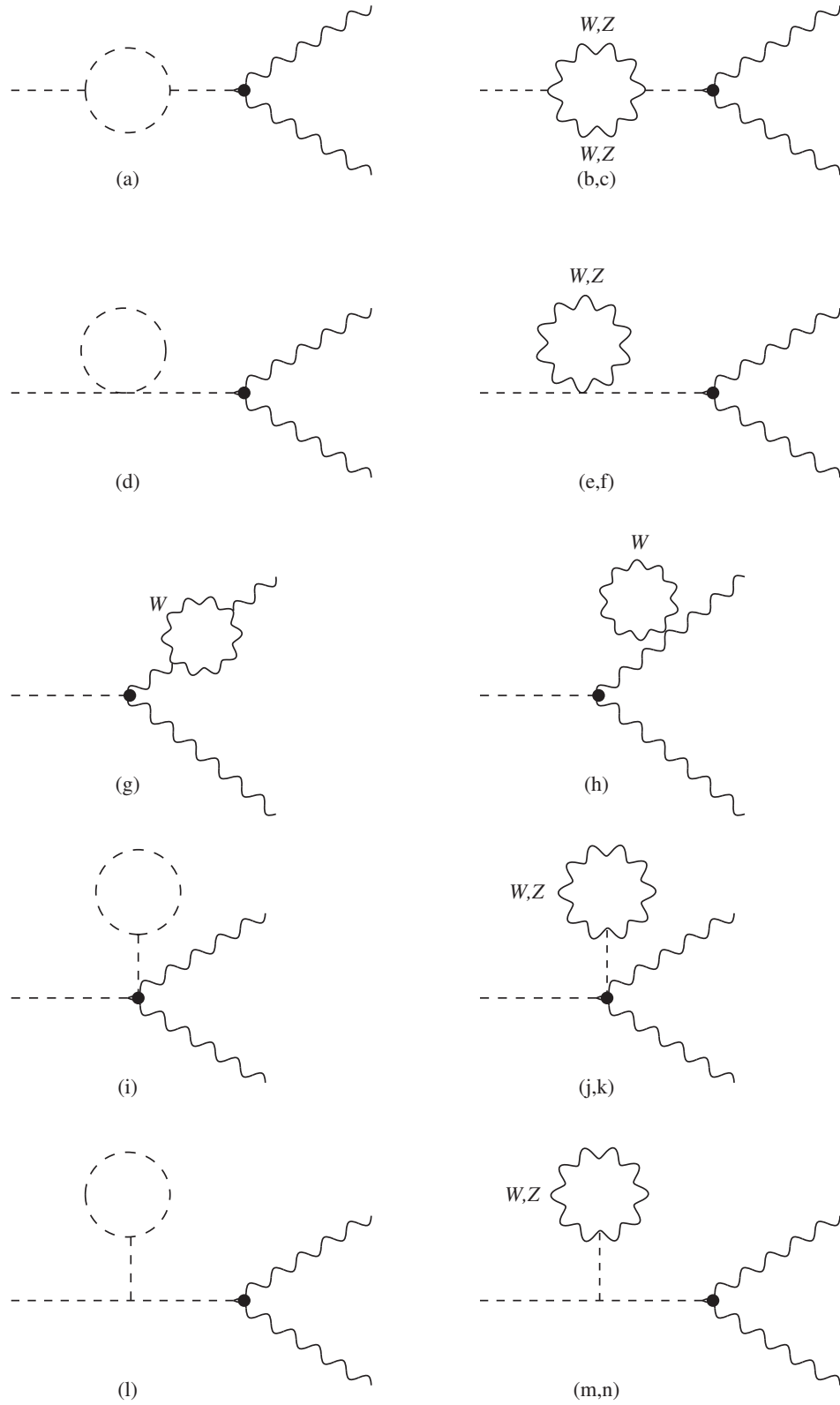


Figure 7.1: One-loop reducible graphs of $H \rightarrow \gamma\gamma$ process

Combination factors due to all possible field contractions in Dyson formula for individual graphs will be:

$$\begin{aligned}
 S_{(a)} &= 36, & S_{(b)} &= 2, & S_{(c)} &= 4, \\
 S_{(d)} &= 12, & S_{(e)} &= 2, & S_{(f)} &= 2, \\
 S_{(g)} &= 36, & S_{(h)} &= 12, & S_{(i)} &= 12.
 \end{aligned} \tag{7.1}$$

Individual terms of $\Sigma(p^2)$ can be simply evaluated by the means of Passarino-Veltman reduction:

$$\text{---} \circ \text{---} = \frac{9g^2mh^4}{128\pi^4mw^2} \frac{1}{[l^2-mh^2]} \frac{1}{[(l+p)^2-mh^2]} = \dots = \frac{9ig^2mh^4B_0(p^2,mh^2,mh^2)}{128\pi^2mw^2}$$

$$\begin{aligned}
 \text{---} \begin{array}{c} w \\ \text{---} \circ \text{---} \end{array} &= \frac{g^2mw^2}{16\pi^4} g^{\alpha\delta} g^{\beta\gamma} \left(\frac{l^\gamma l^\delta}{mw^2} - g^{\gamma\delta} \right) \left(\frac{(l^\alpha+p^\alpha)(l^\beta+p^\beta)}{mw^2} - g^{\alpha\beta} \right) \\
 &\times \frac{1}{[l^2-mw^2]} \frac{1}{[(l+p)^2-mw^2]} = \\
 \dots &= \frac{ig^2((12mw^4-4mw^2p^2+p^4)B_0(p^2,mw^2,mw^2)-2p^2A_0(mw^2))}{64\pi^2mw^2}
 \end{aligned}$$

$$\begin{aligned}
 \text{---} \begin{array}{c} z \\ \text{---} \circ \text{---} \end{array} &= \frac{g^2mz^2}{32\pi^4 \cos^2(\theta_w)} g^{\alpha\delta} g^{\beta\gamma} \left(\frac{l^\gamma l^\delta}{mz^2} - g^{\gamma\delta} \right) \left(\frac{(l^\alpha+p^\alpha)(l^\beta+p^\beta)}{mz^2} - g^{\alpha\beta} \right) \\
 &\times \frac{1}{[l^2-mz^2]} \frac{1}{[(l+p)^2-mz^2]} = \\
 \dots &= \frac{ig^2((12mz^4-4mz^2p^2+p^4)B_0(p^2,mz^2,mz^2)-2p^2A_0(mz^2))}{128\pi^2mz^2 \cos^2(\theta_w)}
 \end{aligned}$$

$$\text{---} \circ \text{---} = \frac{3g^2mh^2}{128\pi^4mw^2} \frac{1}{[l^2-mh^2]} = \dots = \frac{3ig^2mh^2A_0(mh^2)}{128\pi^2mw^2}$$

$$\text{---} \begin{array}{c} w \\ \text{---} \circ \text{---} \end{array} = -\frac{g^2}{32\pi^4} g^{\alpha\beta} \left(\frac{l^\alpha l^\beta}{mw^2} - g^{\alpha\beta} \right) \frac{1}{[l^2-mw^2]} = \dots = \frac{3ig^2A_0(mw^2)}{32\pi^2}$$

$$\begin{aligned}
 \begin{array}{c} z \\ \text{---} \end{array} \text{---} \text{---} &= -\frac{g^2}{64\pi^4 \cos^2(\theta_w)} g^{\alpha\beta} \left(\frac{l^\alpha l^\beta}{mz^2} - g^{\alpha\beta} \right) \frac{1}{[l^2 - mz^2]} = \dots = \frac{3ig^2 A_0(mz^2)}{64\pi^2 \cos^2(\theta_w)} \\
 \begin{array}{c} \text{---} \\ \text{---} \end{array} \text{---} &= \frac{9g^2 mh^4}{128\pi^4 mw^2} \frac{1}{[0 - mh^2]} \frac{1}{[l^2 - mh^2]} = \dots = -\frac{9ig^2 mh^2 A_0(mh^2)}{128\pi^2 mw^2} \\
 \begin{array}{c} w \\ \text{---} \end{array} \text{---} &= -\frac{3g^2 mh^2 g^{\alpha\beta} \left(\frac{l^\alpha l^\beta}{mw^2} - g^{\alpha\beta} \right) \frac{1}{[0 - mh^2]} \frac{1}{[l^2 - mw^2]}}{32\pi^4} = \dots = -\frac{9ig^2 A_0(mw^2)}{32\pi^2} \\
 \begin{array}{c} z \\ \text{---} \end{array} \text{---} &= -\frac{3g^2 mh^2 mz^2 g^{\alpha\beta} \left(\frac{l^\alpha l^\beta}{mz^2} - g^{\alpha\beta} \right) \frac{1}{[0 - mh^2]} \frac{1}{[l^2 - mz^2]}}{64\pi^4 mw^2} = \dots = -\frac{9ig^2 mz^2 A_0(mz^2)}{64\pi^2 mw^2}
 \end{aligned}$$

Summing it all together, we get:

$$\begin{aligned}
 \Sigma(p^2) &= \frac{ig^2}{128\pi^2 m_W^2} \left[9m_H^4 B_0(p^2, m_H^2, m_H^2) + 2p^4 B_0(p^2, m_W^2, m_W^2) \right. \\
 &\quad - 8m_W^2 p^2 B_0(p^2, m_W^2, m_W^2) + 24m_W^4 B_0(p^2, m_W^2, m_W^2) + p^4 B_0(p^2, m_Z^2, m_Z^2) \\
 &\quad - 4mz^2 p^2 B_0(p^2, m_Z^2, m_Z^2) + 12m_Z^4 B_0(p^2, m_Z^2, m_Z^2) - 6m_H^2 A_0(m_H^2) \\
 &\quad \left. - 4(6m_W^2 + p^2) A_0(m_W^2) - 2p^2 A_0(m_Z^2) - 12m_Z^2 A_0(m_Z^2) \right]. \tag{7.2}
 \end{aligned}$$

Applying relations (A.5) and (A.6) for Passarino-Veltman scalar integrals, we get:

$$\begin{aligned}
 \Sigma(p^2) = & \frac{1}{128\pi^2 m_W^2} i g^2 \left[9m_H^4 \left(\sqrt{1 - \frac{4m_H^2}{p^2}} \log \frac{\sqrt{1 - \frac{4m_H^2}{p^2}} - 1}{\sqrt{1 - \frac{4m_H^2}{p^2}} + 1} - \log \frac{m_H^2}{\mu^2} + \frac{1}{\epsilon} + 2 \right) \right. \\
 & + 6m_H^4 \left(\log \frac{m_H^2}{\mu^2} - \frac{1}{\epsilon} - 1 \right) + 2p^4 \left(\sqrt{1 - \frac{4m_W^2}{p^2}} \log \frac{\sqrt{1 - \frac{4m_W^2}{p^2}} - 1}{\sqrt{1 - \frac{4m_W^2}{p^2}} + 1} - \log \frac{m_W^2}{\mu^2} \right. \\
 & \left. \left. + \frac{1}{\epsilon} + 2 \right) - 8m_W^2 p^2 \left(\sqrt{1 - \frac{4m_W^2}{p^2}} \log \frac{\sqrt{1 - \frac{4m_W^2}{p^2}} - 1}{\sqrt{1 - \frac{4m_W^2}{p^2}} + 1} - \log \frac{m_W^2}{\mu^2} + \frac{1}{\epsilon} + 2 \right) \right. \\
 & + 4m_W^2 (6m_W^2 + p^2) \left(\log \frac{m_W^2}{\mu^2} - \frac{1}{\epsilon} - 1 \right) + 24m_W^4 \left(\sqrt{1 - \frac{4m_W^2}{p^2}} \log \frac{\sqrt{1 - \frac{4m_W^2}{p^2}} - 1}{\sqrt{1 - \frac{4m_W^2}{p^2}} + 1} \right. \\
 & \left. - \log \frac{m_W^2}{\mu^2} + \frac{1}{\epsilon} + 2 \right) + p^4 \left(\sqrt{1 - \frac{4m_Z^2}{p^2}} \log \frac{\sqrt{1 - \frac{4m_Z^2}{p^2}} - 1}{\sqrt{1 - \frac{4m_Z^2}{p^2}} + 1} - \log \frac{m_Z^2}{\mu^2} + \frac{1}{\epsilon} + 2 \right) \\
 & - 4m_Z^2 p^2 \left(\sqrt{1 - \frac{4m_Z^2}{p^2}} \log \frac{\sqrt{1 - \frac{4m_Z^2}{p^2}} - 1}{\sqrt{1 - \frac{4m_Z^2}{p^2}} + 1} - \log \frac{m_Z^2}{\mu^2} + \frac{1}{\epsilon} + 2 \right) \\
 & + 2m_Z^2 p^2 \left(\log \frac{m_Z^2}{\mu^2} - \frac{1}{\epsilon} - 1 \right) + 12m_Z^4 \left(\sqrt{1 - \frac{4m_Z^2}{p^2}} \log \frac{\sqrt{1 - \frac{4m_Z^2}{p^2}} - 1}{\sqrt{1 - \frac{4m_Z^2}{p^2}} + 1} \right. \\
 & \left. \left. - \log \frac{m_Z^2}{\mu^2} + \frac{1}{\epsilon} + 2 \right) + 12m_Z^4 \left(\log \frac{m_Z^2}{\mu^2} - \frac{1}{\epsilon} - 1 \right) \right]. \tag{7.3}
 \end{aligned}$$

We can now perform Taylor expansion around $p^2 = m_H^2$:

$$\Sigma(p^2) = A + B(p^2 - m_H^2) + C(p^2 - m_H^2)^2 + O(p^2 - m_H^2)^3. \tag{7.4}$$

Factor of each order A, B, C is going to have finite and infinite parts:

$$\begin{aligned}
 A &= F_A + I_A \\
 B &= F_B + I_B \\
 C &= F_C + I_C
 \end{aligned} \tag{7.5}$$

with:

$$I_A = \frac{3ig^2 m_H^2 (m_H^2 - 2m_W^2 - m_Z^2)}{64\pi^2 m_W^2 \epsilon} \quad (7.6)$$

$$\begin{aligned} F_A = & -\frac{1}{128\pi^2 m_W^2} ig^2 \left[2m_H^4 \log \frac{m_W^2}{\mu^2} + m_H^4 \log \frac{m_Z^2}{\mu^2} + 3\sqrt{3}\pi m_H^4 - 18m_H^4 \right. \\ & - 12m_H^2 m_W^2 \log \frac{m_W^2}{\mu^2} + 20m_H^2 m_W^2 - 6m_H^2 m_Z^2 \log \frac{m_Z^2}{\mu^2} + 10m_H^2 m_Z^2 \\ & - 2\sqrt{1 - \frac{4m_W^2}{m_H^2}} (m_H^4 - 4m_H^2 m_W^2 + 12m_W^4) \log \frac{\sqrt{1 - \frac{4m_W^2}{m_H^2}} - 1}{\sqrt{1 - \frac{4m_W^2}{m_H^2}} + 1} \\ & - \sqrt{1 - \frac{4m_Z^2}{m_H^2}} (m_H^4 - 4m_H^2 m_Z^2 + 12m_Z^4) \log \frac{\sqrt{1 - \frac{4m_Z^2}{m_H^2}} - 1}{\sqrt{1 - \frac{4m_Z^2}{m_H^2}} + 1} \\ & \left. + 3m_H^4 \log \frac{m_H^2}{\mu^2} - 24m_W^4 - 12m_Z^4 \right] \quad (7.7) \end{aligned}$$

$$I_B = \frac{3ig^2 (m_H^2 - 2m_W^2 - m_Z^2)}{64\pi^2 m_W^2 \epsilon} \quad (7.8)$$

$$\begin{aligned} F_B = & \frac{1}{128\pi^2 m_H^4 m_W^2 m_Z^2 \sqrt{1 - \frac{4m_W^2}{m_H^2}} \sqrt{1 - \frac{4m_Z^2}{m_H^2}}} \left\{ ig^2 m_Z^2 \sqrt{1 - \frac{4m_W^2}{m_H^2}} \left[m_H^2 \sqrt{1 - \frac{4m_Z^2}{m_H^2}} \right. \right. \\ & \times \left(3(m_H^4 - 2m_H^2 m_Z^2 - 4m_Z^4) - 2(m_H^4 - 3m_H^2 m_Z^2) \log \frac{m_Z^2}{\mu^2} \right) + 2(m_H^6 - 5m_H^4 m_Z^2 \\ & + 4m_H^2 m_Z^4 + 12m_Z^6) \log \frac{\sqrt{1 - \frac{4m_Z^2}{m_H^2}} - 1}{\sqrt{1 - \frac{4m_Z^2}{m_H^2}} + 1} \left. \right] + ig^2 m_Z^2 \sqrt{1 - \frac{4m_Z^2}{m_H^2}} \left[m_H^2 \sqrt{1 - \frac{4m_W^2}{m_H^2}} \right. \\ & \times \left(2\sqrt{3}\pi m_H^4 - 4m_H^2 (m_H^2 - 3m_W^2) \log \frac{m_W^2}{\mu^2} - 3(m_H^4 + 4m_H^2 m_W^2 + 8m_W^4) \right) \\ & \left. \left. + 4(m_H^6 - 5m_H^4 m_W^2 + 4m_H^2 m_W^4 + 12m_W^6) \log \frac{\sqrt{1 - \frac{4m_W^2}{m_H^2}} - 1}{\sqrt{1 - \frac{4m_W^2}{m_H^2}} + 1} \right] \right\} \quad (7.9) \end{aligned}$$

$$\begin{aligned}
 I_C &= \frac{3ig^2}{128\pi^2 m_W^2 \varepsilon} \\
 F_C &= -\frac{ig^2}{768\pi^2 m_H^4 m_W^2} \left\{ \frac{1}{(m_H^2 - 4m_W^2)^2} \left[(m_H^2 - 4m_W^2) \left((8\sqrt{3}\pi - 51) m_H^6 \right. \right. \right. \\
 &\quad \left. \left. \left. - 32 \left(\sqrt{3}\pi - 6 \right) m_H^4 m_W^2 - 24m_H^2 m_W^4 + 12m_H^4 (m_H^2 - 4m_W^2) \log \frac{m_W^2}{\mu^2} + 432m_W^6 \right) \right. \right. \\
 &\quad \left. \left. - 12\sqrt{1 - \frac{4m_W^2}{m_H^2}} (m_H^8 - 6m_H^6 m_W^2 + 6m_H^4 m_W^4 - 16m_H^2 m_W^6 + 72m_W^8) \log \frac{\sqrt{1 - \frac{4m_W^2}{m_H^2}} - 1}{\sqrt{1 - \frac{4m_W^2}{m_H^2}} + 1} \right] \right. \\
 &\quad \left. - \frac{3}{(m_H^2 - 4m_Z^2)^2} \left[m_H^8 - 6m_H^6 m_Z^2 + 12m_H^4 m_Z^4 - 88m_H^2 m_Z^6 - 2m_H^4 (m_H^2 - 4m_Z^2)^2 \right. \right. \\
 &\quad \left. \left. \times \log \frac{m_Z^2}{\mu^2} + 2\sqrt{1 - \frac{4m_Z^2}{m_H^2}} (m_H^8 - 6m_H^6 m_Z^2 + 6m_H^4 m_Z^4 - 16m_H^2 m_Z^6 + 72m_Z^8) \right. \right. \\
 &\quad \left. \left. \times \log \frac{\sqrt{1 - \frac{4m_Z^2}{m_H^2}} - 1}{\sqrt{1 - \frac{4m_Z^2}{m_H^2}} + 1} + 288m_Z^8 \right] \right\}. \tag{7.10}
 \end{aligned}$$

Following the *on-shell* renormalization scheme, i.e. what is usually meant by *on-shell* renormalization of self-energy and propagator corrections in quantum field theories, our goal will be to cancel the first two terms in (7.4) completely. What does it mean physically and the essence of this on-shell renormalization scheme, we are going to discuss in a minute. Our renormalized $\Sigma(p^2)$ will then read:

$$\bar{\Sigma}(p^2) = C(p^2 - m_H^2)^2 + O(p^2 - m_H^2)^3. \tag{7.11}$$

If we now add $\bar{\Sigma}(p^2)$ as a correction to the external line, we get expression that is proportional to:

$$\begin{aligned}
 \bar{\Sigma}(p^2) \cdot \frac{i}{p^2 - m_H^2} &= C(p^2 - m_H^2)^2 \frac{i}{p^2 - m_H^2} + O(p^2 - m_H^2)^3 \\
 &= C(p^2 - m_H^2) + O(p^2 - m_H^2)^3 \tag{7.12}
 \end{aligned}$$

which will give zero for $p^2 \rightarrow m_H^2$. That will make graphs (a) through (n) equal to zero, as we stated in the beginning of this chapter. We have not removed the I_C term in (7.5), but that is ok, since it is a regularized expression and (7.12) will still be zero for $p^2 \rightarrow m_H^2$. Thus, the I_C term does not really bother us here. One remark would be appropriate at this place: in *U-gauge* calibration we are working, we get quartic divergences in vector boson sector due to “bad” behaviour of propagators that cause I_C term, while in *R-gauge* we would only have quadratic divergences so that C term in (7.11) would solely have the finite

part. It suggests a calibration non-invariance of Higgs self-energy in SM, which is a well known fact.

Kinetic and mass terms in SM Lagrangian are

$$\mathcal{L}_{kin}^{SM} + \mathcal{L}_{mass}^{SM} = \frac{1}{2}\partial_\mu H \partial^\mu H - \frac{1}{2}m_H^2 H^2 \quad (7.13)$$

and for the elimination of the first two terms in (7.4), we are going to need the counterterms

$$\mathcal{L}_{CT}^{(Higgs)} = \frac{1}{2}K_2 \partial_\mu H \partial^\mu H - \frac{1}{2}K_1 H^2. \quad (7.14)$$

Summing together $\Sigma(p^2)$ and the two counterterms (treated as interactions), we get

$$\begin{aligned} & \Sigma(p^2) + K_2 p^2 - K_1 = \\ & = A + B(p^2 - m_H^2) + C(p^2 - m_H^2)^2 + O(p^2 - m_H^2)^3 + K_2 p^2 - K_1. \end{aligned} \quad (7.15)$$

Renormalization requirements:

$$A - B m_H^2 - K_1 = 0 \quad (7.16)$$

$$K_2 + B = 0 \quad (7.17)$$

will give renormalization conditions:

$$K_1 = A - B m_H^2 \quad (7.18)$$

$$K_2 = -B \quad (7.19)$$

which will in turn yield Higgs mass and wave function renormalization:

$$\mathcal{L}^{(Higgs)} = \frac{1}{2}(1 + K_2)\partial_\mu H \partial^\mu H - \frac{1}{2}(m_H^2 + K_1)H^2. \quad (7.20)$$

Let us denote

$$1 + K_2 = 1 - B = Z_2. \quad (7.21)$$

We will write the wave function renormalization factor as

$$Z_2^{1/2} H = H_0. \quad (7.22)$$

We can subsequently rewrite (7.20) as

$$\begin{aligned} \mathcal{L}^{(Higgs)} &= \frac{1}{2}\partial_\mu H_0 \partial^\mu H_0 - \frac{1}{2}(m_H^2 + K_1)Z_2^{-1}H_0^2 \\ &= \frac{1}{2}\partial_\mu H_0 \partial^\mu H_0 - \frac{1}{2}(m_H^2 + A - m_H^2 B)(1 + B)H_0^2 = \end{aligned}$$

$$= \frac{1}{2} \partial_\mu H_0 \partial^\mu H_0 - \frac{1}{2} (m_H^2 + A) H_0^2, \quad (7.23)$$

where we have omitted terms AB and $m_H^2 B^2$ which are of the order of g^4 , so we can ignore them against A which is of the order of g^2 . We set

$$m_{0H}^2 = m_H^2 + A \quad (7.24)$$

and we can write the bare Lagrangian as:

$$\mathcal{L}^{(Higgs)} = \frac{1}{2} \partial_\mu H_0 \partial^\mu H_0 - \frac{1}{2} m_{0H}^2 H_0^2, \quad (7.25)$$

with H_0 standing for the bare wave function and m_{0H} representing the bare mass. To achieve consistency, we perform the field renormalization through the entire Lagrangian, but we can formally absorb the unwanted counterterms that appear in other interaction terms into the redefinition of bare coupling constants in the following manner:

$$f^i H_0^3 = f^i Z_2^{3/2} H^3 \rightarrow f_0^i H_0^3 = f^i H^3 \quad (7.26)$$

with

$$f_0^i = f^i Z_2^{-3/2}. \quad (7.27)$$

The same way it also works for the mass counterterm in (7.25).

We will now discuss the promised “on-shellness”, represented by a cancellation of the first two terms in (7.4). One-loop correction to Higgs field propagator will read as:

$$\begin{aligned} & \frac{i}{p^2 - m_H^2} + \frac{i}{p^2 - m_H^2} \cdot i \Sigma(p^2) \frac{i}{p^2 - m_H^2} = \\ & = \frac{i}{p^2 - m_H^2 + \Sigma(p^2)} - \text{terms of higher order of perturbation expansion.} \end{aligned} \quad (7.28)$$

By “terms of higher order of perturbation expansion” we mean two and more loop corrections of Higgs propagator. So, within our order of perturbation expansion, we can assume

$$\begin{aligned} & \frac{i}{p^2 - m_H^2} + \frac{i}{p^2 - m_H^2} \cdot i \Sigma(p^2) \frac{i}{p^2 - m_H^2} = \\ & = \frac{i}{p^2 - m_H^2 + \Sigma(p^2)}. \end{aligned} \quad (7.29)$$

If we use the renormalization scheme $\Sigma(p^2) \rightarrow \bar{\Sigma}(p^2)$, according to (7.11), we get:

$$\begin{aligned} \frac{i}{p^2 - m_H^2 + \bar{\Sigma}(p^2)} &= \frac{i}{p^2 - m_H^2 + C(p^2 - m_H^2)^2 + \dots} = \\ &= \frac{i}{p^2 - m_H^2(1 + C(p^2 - m_H^2) + \dots)} = \frac{i}{p^2 - m_H^2} \left[1 - C(p^2 - m_H^2) + \dots \right]. \end{aligned} \quad (7.30)$$

Such corrected propagator has two unique properties caused by this particular renormalization scheme:

- It has a pole in the physical mass m_H
- It has a residue 1

As a result, an entity renormalized in such way has the same properties and the same analytical structure as a free-field propagator, hence the tag “*on-shell*”.

7.2 One-loop corrections to the external Photon line

In much the same way we are going to deal with graphs (g) and (h) of Fig. 7.1, meaning we are going to employ the “on-shell” scheme for photons. First, we calculate:

$$i\Pi(p) = \text{(g)} + \text{(h)}$$

The image shows two Feynman diagrams labeled (g) and (h). Diagram (g) is a photon line (wavy) with a W boson loop (curly) attached to it. Diagram (h) is a photon line (wavy) with a ghost loop (curly) attached to it. The diagrams are summed together to represent the self-energy correction $i\Pi(p)$.

After a series of steps just like in previous case, we get the result:

$$i\Pi(p) = i(p^2 g^{\mu\nu} - p^\mu p^\nu) \Pi(p^2) \quad (7.31)$$

with:

$$\begin{aligned} \Pi(p^2) &= \frac{1}{36m_W^4 p^2} i\pi^2 e^2 \left[3(4m_W^2 - p^2)(12m_W^4 + 20m_W^2 p^2 + p^4) \right. \\ &\quad \cdot \left. \left(\sqrt{1 - \frac{4m_W^2}{p^2}} \log \frac{\sqrt{1 - \frac{4m_W^2}{p^2}} - 1}{\sqrt{1 - \frac{4m_W^2}{p^2}} + 1} - \log \frac{m_W^2}{\mu^2} + \frac{1}{\epsilon} + 2 \right) \right] \end{aligned}$$

$$\begin{aligned} & \cdot \left(-6m_W^2 (-24m_W^4 + 8m_W^2 p^2 + p^4) \left(\log \frac{m_W^2}{\mu^2} - \frac{1}{\epsilon} - 1 \right) \right. \\ & \left. + 2 (6m_W^2 - p^2) (12m_W^4 - 4m_W^2 p^2 + p^4) \right). \end{aligned} \quad (7.32)$$

We define renormalized Π as

$$\bar{\Pi}(p^2) = \Pi(p^2) - \Pi(0) \quad (7.33)$$

with $\Pi(0)$ congaing the divergent part

$$\Pi(0) = \frac{7i\pi^2 e^2}{\epsilon} - 7i\pi^2 e^2 \log \frac{m_W^2}{\mu^2}. \quad (7.34)$$

So, (7.31) becomes $i\Pi(p) = i(p^2 g^{\mu\nu} - p^\mu p^\nu)(\Pi(p^2) - \Pi(0) + \Pi(0))$ and we will require counterterm

$$(p^2 g^{\mu\nu} - p^\mu p^\nu) K_3 \quad (7.35)$$

with $K_3 = -\Pi(0)$. (7.35) can be acquired from the electromagnetic kinetic term of SM Lagrangian:

$$\begin{aligned} \mathcal{L}^{EM} + \mathcal{L}_{CT}^{EM} &= -\frac{1}{4} F_{\mu\nu} F^{\mu\nu} - \frac{1}{4} K_3 F_{\mu\nu} F^{\mu\nu} = -\frac{1}{4} (1 + K_3) F_{\mu\nu} F^{\mu\nu} \\ &= -\frac{1}{4} Z_3 F_{\mu\nu} F^{\mu\nu}, \end{aligned} \quad (7.36)$$

with $F_{\mu\nu} = \partial_\mu A_\nu - \partial_\nu A_\mu$, and will yield photon wave function renormalization

$$A_0^\mu = Z_3^{1/2} A^\mu. \quad (7.37)$$

The bare Lagrangian will read as:

$$\mathcal{L}^{EM} = -\frac{1}{4} F_{0\mu\nu} F_0^{\mu\nu}. \quad (7.38)$$

Graphs with corrections on the external lines in this renormalization scheme will be canceled in the following way: Correction on the external line is

$$\frac{g_{\alpha\mu}}{p^2} \bar{\Pi}(p^2) (p^2 g^{\mu\nu} - p^\mu p^\nu) \varepsilon_\nu(p). \quad (7.39)$$

Second term gets canceled by the means of relation $p^\nu \varepsilon_\nu(p) = 0$, valid for all vector bosons. First term gets canceled as well in case of on-shell photon, since we can easily see that

$$\bar{\Pi}(p^2 \rightarrow 0) = 0 \quad (7.40)$$

One-loop corrected propagator in this renormalization scheme will be

$$-i\frac{g_{\alpha\beta}}{p^2} + -i\frac{g_{\alpha\mu}}{p^2} (-i)\bar{\Pi}(p^2) (p^2 g^{\mu\nu} - p^\mu p^\nu) \cdot (-i\frac{g_{\nu\beta}}{p^2}). \quad (7.41)$$

For the case of on-shell photon ($p^2 \rightarrow 0$), such one-loop corrected propagator will be proportional to

$$-i\frac{g_{\alpha\beta}}{p^2}, \quad (7.42)$$

just like in free case.

7.3 One-loop vertex corrections

Thanks to employing this renormalization scheme, we have canceled all graphs on Fig. 7.1 that contain one-loop corrections of the external lines. So, the only graphs that remain to be calculated, are vertex corrections (i), (j), and (k):

$$i\mathcal{M}_{H\gamma\gamma(i)}^{red} = \frac{3ie^2g}{128\pi^2m_W} A_0(m_H^2) (f_{BB}^\Lambda - f_{BW}^\Lambda + f_{WW}^\Lambda) (m_H^2g^{\mu\nu} - 2k^\mu p^\nu) \quad (7.43)$$

$$i\mathcal{M}_{H\gamma\gamma(j)}^{red} = \frac{3ie^2gm_W}{32\pi^2m_H^2} A_0(m_W^2) (f_{BB}^\Lambda - f_{BW}^\Lambda + f_{WW}^\Lambda) (m_H^2g^{\mu\nu} - 2k^\mu p^\nu) \quad (7.44)$$

$$i\mathcal{M}_{H\gamma\gamma(k)}^{red} = \frac{3ie^2gm_Z}{64\pi^2m_H^2 \cos(\theta_W)} A_0(m_Z^2) (f_{BB}^\Lambda - f_{BW}^\Lambda + f_{WW}^\Lambda) \\ \times (m_H^2g^{\mu\nu} - 2k^\mu p^\nu). \quad (7.45)$$

Summing the previous three amplitudes together, we get the result for all one-loop reducible graphs of $H \rightarrow \gamma\gamma$ process within our effective electroweak theory:

$$i\mathcal{M}_{H\gamma\gamma}^{red(eff)} = \frac{3ie^2g}{128\pi^2m_W} (f_{BB}^\Lambda - f_{BW}^\Lambda + f_{WW}^\Lambda) \left(g^{\mu\nu} - \frac{2k^\mu p^\nu}{m_H^2} \right) \\ \left[m_H^2 A_0(m_H^2) + 4m_W^2 A_0(m_W^2) + 2m_Z^2 A_0(m_Z^2) \right] \\ \times \varepsilon_\mu^*(p) \varepsilon_\nu^*(k). \quad (7.46)$$

Divergent part of the result (7.46) will read as:

$$i\mathcal{M}_{H\gamma\gamma(div)}^{red(eff)} = \frac{3ie^2g}{128\pi^2m_H^2m_W} (m_H^4 + 4m_W^4 + 2m_Z^4) (f_{BB}^\Lambda - f_{BW}^\Lambda + f_{WW}^\Lambda) \\ \times (m_H^2g^{\mu\nu} - 2k^\mu p^\nu) \frac{1}{\varepsilon}. \quad (7.47)$$

The same set of steps as for one-loop irreducible graphs in chapter 6, section 6.2 will yield counterterm renormalization equation:

$$\xi f_{BB} - \xi f_{BW} + \xi f_{WW} = \frac{3g^2}{128\pi^2m_H^2m_W^2} (m_H^4 + 4m_W^4 + 2m_Z^4) \\ \times (f_{BB}^r - f_{BW}^r + f_{WW}^r). \quad (7.48)$$

Put together with equation (6.38), we receive renormalization equation for both reducible and irreducible graphs:

$$\begin{aligned} \xi f_{\text{BB}} - \xi f_{\text{BW}} + \xi f_{\text{WW}} = & \frac{g^2}{128\pi^2 m w^2} \left[2f_B^r (m h^2 - 6m w^2) - 3m h^2 f_{\text{BB}}^r \right. \\ & - m h^2 f_{\text{BW}}^r + 24m w^2 f_{\text{BW}}^r + 288g^2 m w^2 f_{\text{DW}}^r \\ & - 72g^2 m w^2 f_{\text{WWW}}^r + 2m h^2 f_W^r - 3m h^2 f_{\text{WW}}^r \\ & - 12m w^2 f_W^r + 3 \left(m_H^2 + 4 \frac{m_W^4}{m_H^2} + \frac{2m_Z^4}{m_H^2} \right) \\ & \left. \times (f_{\text{BB}}^r - f_{\text{BW}}^r + f_{\text{WW}}^r) \right]. \end{aligned} \quad (7.49)$$

Chapter 8

Discussion of results and conclusion

8.1 Summary of results and discussion

Let us now sum the results of our calculations and focus on physical implications they have. Summing together all our previous results, we obtain:

$$i\mathcal{M}(H \rightarrow \gamma\gamma) = X \left(g^{\mu\nu} - \frac{2k^\mu p^\nu}{m_H^2} \right) \varepsilon_\mu^*(p) \varepsilon_\nu^*(k), \quad (8.1)$$

with:

$$X = e^2 g F_{\text{SM}} + e^2 F_{\text{eff}}^{\text{tree}} + e^2 g F_{\text{eff}}^{\text{loop}}, \quad (8.2)$$

and

$$F_{\text{SM}} = F_{\text{VB}} + F_{\text{top}} \quad (8.3)$$

$$F_{\text{VB}} = \frac{3im_W}{8\pi^2} \left[1 + \frac{m_H^2}{6m_W^2} + (2m_W^2 - m_H^2)C_0(m_H^2, 0, 0, m_W^2, m_W^2, m_W^2) \right] \quad (8.4)$$

$$F_{\text{top}} = \frac{-i}{6\pi^2} \frac{m_t^2}{m_W} \left[2 + (4m_t^2 - m_H^2)C_0(m_H^2, 0, 0, m_t^2, m_t^2, m_t^2) \right] \quad (8.5)$$

$$F_{\text{eff}}^{\text{tree}} = \frac{i m_H^2 m_W}{g} (f_{BB}^\Lambda - f_{BW}^\Lambda + f_{wW}^\Lambda) \quad (8.6)$$

$$F_{\text{eff}}^{\text{loop}} = F^{\text{ired}} + F^{\text{red}} \quad (8.7)$$

$$\begin{aligned}
 F^{\text{ired}} = & -\frac{i}{128m_W\pi^2} \left\{ 8 \left[f_B^\Lambda - 2f_{BW}^\Lambda + f_W^\Lambda + 3g^2(-4f_{DW}^\Lambda + f_{WWW}^\Lambda) \right] m_H^2 m_W^2 B_0(0, m_W^2, m_W^2) \right. \\
 & - 3(f_{BB}^\Lambda - f_{BW}^\Lambda + f_{WW}^\Lambda) m_H^4 B_0(m_H^2, m_H^2, m_H^2) \\
 & + 2 \left[m_H^2 \left((f_B^\Lambda - 2f_{BW}^\Lambda + f_W^\Lambda) m_H^2 - 2(f_B^\Lambda - 2f_{BW}^\Lambda + f_W^\Lambda \right. \right. \\
 & \left. \left. + 12g^2(-4f_{DW}^\Lambda + f_{WWW}^\Lambda) m_W^2 \right) B_0(m_H^2, m_W^2, m_W^2) \right. \\
 & \left. + 4m_W^2 \left[(f_B^\Lambda - 2(f_{BW}^\Lambda + 7g^2 f_{DW}^\Lambda) + 3g^2 f_{WWW}^\Lambda) m_H^2 - 24(g^2 f_{DW}^\Lambda + f_{WW}^\Lambda) m_W^2 \right. \right. \\
 & \left. \left. + 2 \left((f_W^\Lambda - 2f_{WW}^\Lambda) m_H^4 - (f_B^\Lambda - 2f_{BW}^\Lambda + 2(f_W^\Lambda - 7f_{WW}^\Lambda) \right. \right. \right. \\
 & \left. \left. \left. + 3g^2(-8f_{DW}^\Lambda + f_{WWW}^\Lambda) m_H^2 m_W^2 - 36(g^2 f_{DW}^\Lambda + f_{WW}^\Lambda) m_W^4 \right) \right. \right. \\
 & \left. \left. \times C_0(m_H^2, 0, 0; m_W^2, m_W^2, m_W^2) \right. \right. \\
 & \left. \left. + 4(g^2 f_{DW}^\Lambda + f_{WW}^\Lambda) m_W^2 \left(-(m_H^2 + 6m_W^2) C_0(m_H^2, m_H^2, 0; m_W^2, m_W^2, m_W^2) \right. \right. \right. \\
 & \left. \left. \left. - 2m_W^2(-m_H^2 + 6m_W^2)(D_0(m_H^2; m_W^2) + 2D_0(m_H^2, m_H^2; m_W^2)) \right) \right] \right\}, \\
 F^{\text{red}} = & \frac{3i}{128\pi^2 m_W} (f_{BB}^\Lambda - f_{BW}^\Lambda + f_{WW}^\Lambda) \\
 & \times \left[m_H^2 A_0(m_H^2) + 4m_W^2 A_0(m_W^2) + 2m_Z^2 A_0(m_Z^2) \right]. \tag{8.8}
 \end{aligned}$$

The corresponding decay rate is given by:

$$\Gamma(H \rightarrow \gamma\gamma) = \frac{8\pi\alpha^2 G_F m_W^2}{\sqrt{2} m_H} |F_{\text{SM}} + \frac{1}{g} F_{\text{eff}}^{\text{tree}} + F_{\text{eff}}^{\text{loop}}|^2. \tag{8.9}$$

We can see that our summary result (8.1) exhibits the desired transverse tensor structure, as we have discussed in chapter 3.

Looking back at the result (8.8), one can see that it contains a lot of unknown free parameters, which makes it difficult to make any specific prediction of the SM decay rate correction, whatsoever. Nevertheless, it is interesting to discuss several physical implications depending on the values of constants f_i , Higgs mass and the scale of the new physics Λ . As we have discussed in Chapter 1, a general scale of the new physics would be somewhere around $\Lambda = 1$ TeV. First, we will discuss the value of the $H \rightarrow \gamma\gamma$ decay rate as a function of Higgs boson mass. In Fig. 8.1, we discuss how dimension-six operators affect the original SM decay rate of $H \rightarrow \gamma\gamma$. In the first plot, we set all constants f_i equal to 1, which

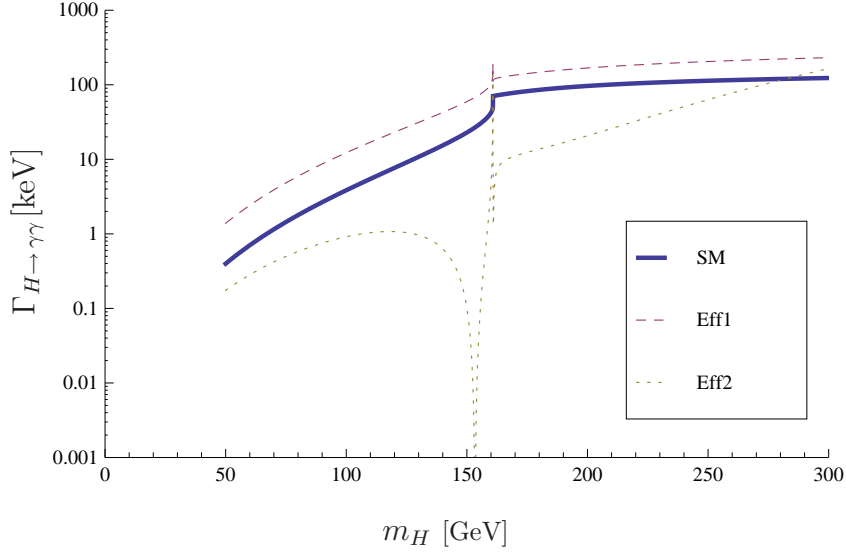


Figure 8.1: Dimension-six bosonic operators contribution to $\Gamma_{H\rightarrow\gamma\gamma}$ at $\Lambda = 1$ TeV, SM curve represents pure Standard Model contribution, Eff1 shows SM decay rate enhancement by effective theory for all $f_i = 1$, Eff2 represents special choice of constants: $f_{WW} = 1.7$, $f_{BB} = -6.5$, $f_{BW} = -3$, $f_{DW} = 5.2$, $f_{WWW} = 5.5$, $f_B = -4$ and $f_W = 8.5$, which leads to SM decay rate reduction.

leads to the enhancement of SM decay rate, in the second plot we introduce such choice of constants f_i that will roughly suppress the SM rate, especially within the domain of today's expected Higgs mass: 100 - 200 GeV.

In Fig. 8.2, we show how positive constants f_i boost the SM decay rate. In Fig. 8.3, we can see the opposite effect - negative constants f_i decrease the SM decay rate. Fig 8.4 shows more or less random choice of f_i , and we can see that it can lead to both, significant enhancement of SM decay rate, or its substantial reduction.

We expect that the leading contribution of dimension-six operators would come from the tree level (8.6). Fig. 8.5 confirms that this is true: In the event of accidental tree-level suppression ($f_{BB} - f_{BW} + f_{WW} \rightarrow 0$), while all other f_i are kept equal to 1, so we can say that almost all f_i 's are of the same magnitude, we can see from curve (I) that one-loop dimension-six diagrams contribution is rather small, especially within the expected Higgs mass domain. However, curves (II) and (III) show us that although the tree level is suppressed, one-loop diagrams can become significant if the appropriate constants are increased accordingly. It is also interesting to notice that tree-level contribution is strictly dominant in the domain of $m_H < 160$ GeV, and with tree level suppressed, we fail to alter the decay rate significantly with any sets of the remaining constants f_i . A half dozen other sets, aside those we see on fig. 8.5, have been tried and they do confirm this observation.

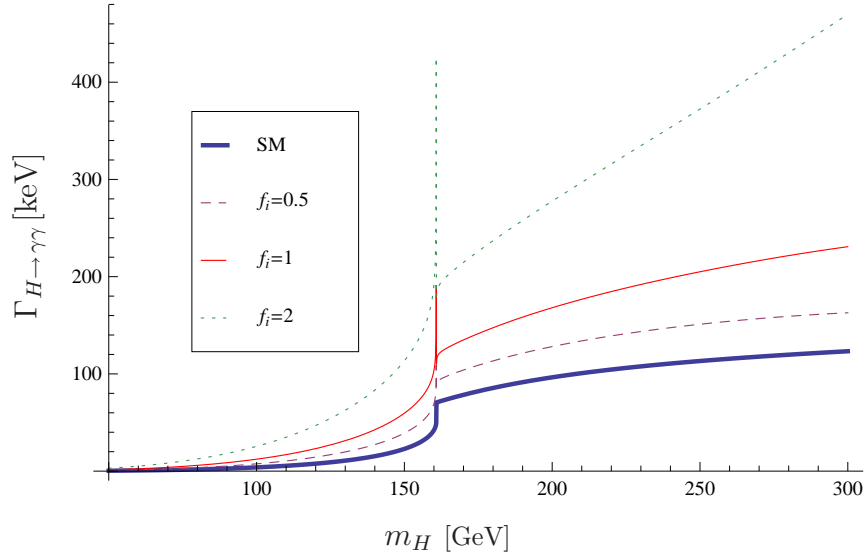


Figure 8.2: SM decay rate gets enhanced for increasing values of f'_i 's

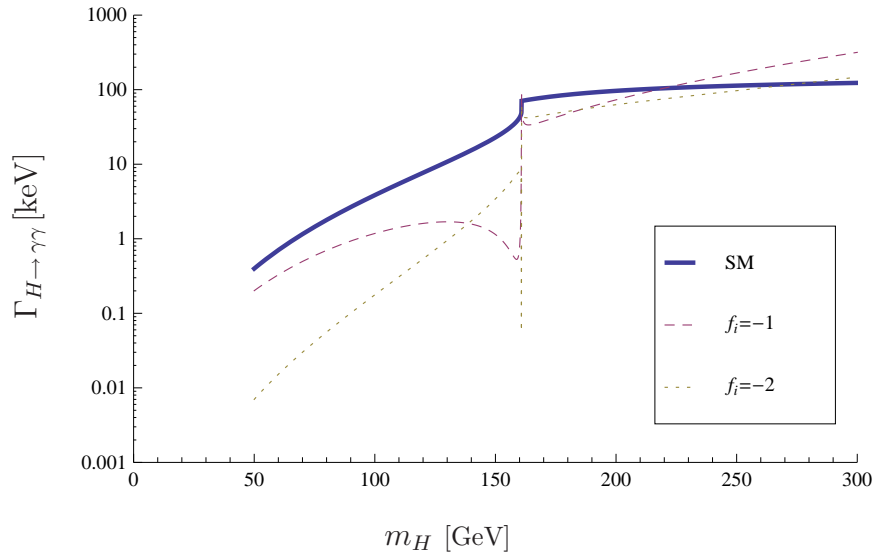


Figure 8.3: SM decay rate gets dampened for negative values of f'_i 's

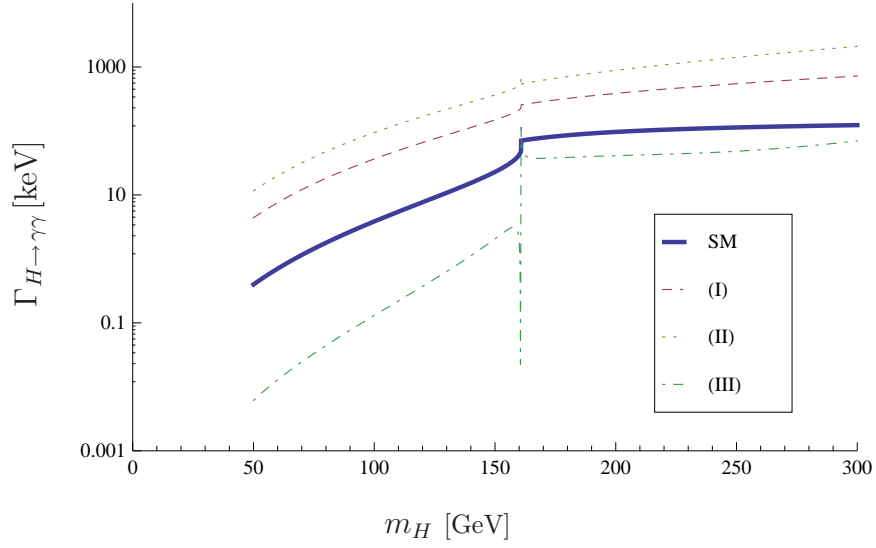


Figure 8.4: Random dispersion of f'_i 's. (I): $f_{WW} = 0.5$, $f_{BB} = 1$, $f_{BW} = -1$, $f_{DW} = -1.2$, $f_{WWW} = 1.5$, $f_B = -0.7$, $f_W = 2.2$, (II): $f_{WW} = 2$, $f_{BB} = 1.3$, $f_{BW} = -1.5$, $f_{DW} = -1.7$, $f_{WWW} = 0.5$, $f_B = -1$, $f_W = 0.5$, (III): $f_{WW} = -5$, $f_{BB} = 5$, $f_{BW} = 1$, $f_{DW} = 1.2$, $f_{WWW} = -2$, $f_B = 1.2$, $f_W = 2.3$

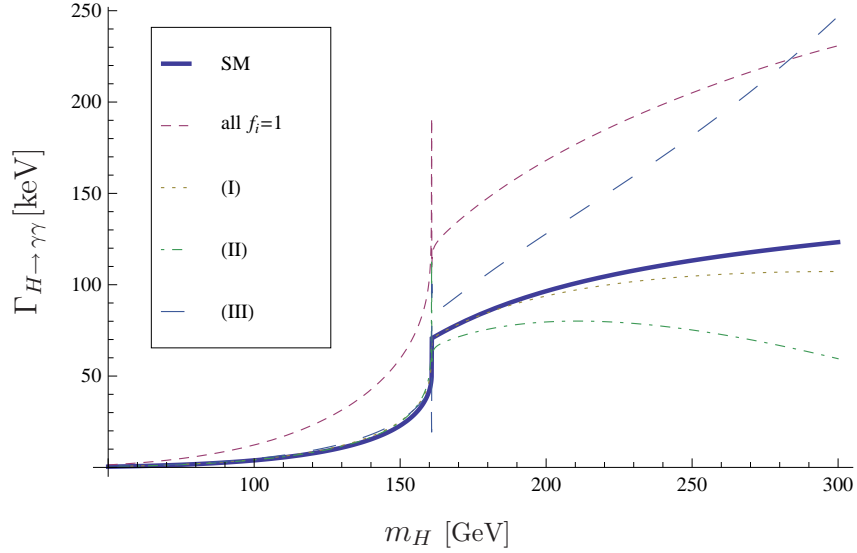


Figure 8.5: Tree-level contribution and the significance of one-loop diagrams: (I): $(f_{BB} - f_{BW} + f_{WW} \rightarrow 0)$ while all other $f_i = 1$, (II): $(f_{BB} - f_{BW} + f_{WW} \rightarrow 0)$ while all other $f_i = 3$, (III): $(f_{BB} - f_{BW} + f_{WW} \rightarrow 0)$ while all other $f_i = -3$.

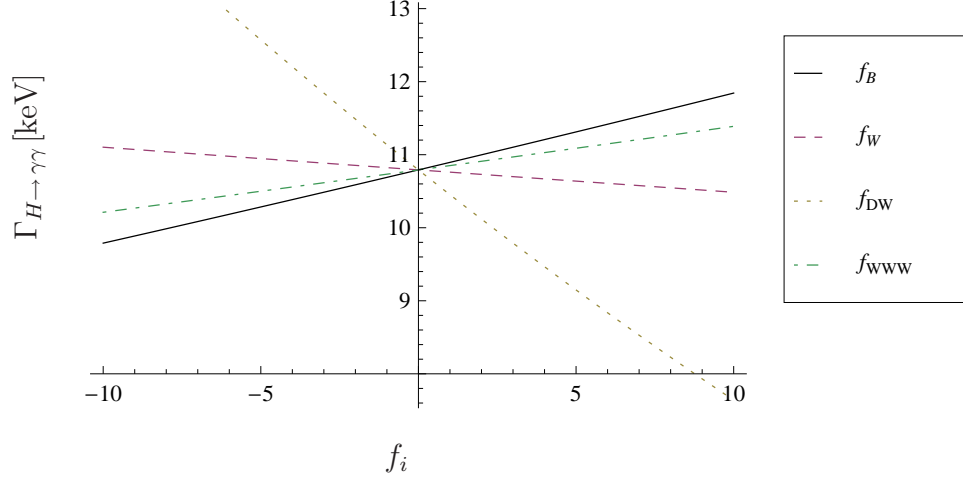


Figure 8.6: Significance of individual constants f_i : $f_{BB} - f_{BW} + f_{WW}$ is set close to zero, we see the dependence on individual coefficients f_i with the rest of them being set to zero. $m_H = 130$ GeV, $\Lambda = 1$ TeV.

We could also speculate how much is the entire process dependent upon individual constants f_i [3]. It has already been seen that constants f_{BB} , f_{BW} and f_{WW} play the dominant role, due to involvement in the tree-level contribution. Apart from that, it would also be interesting to look at the others. So, let us again assume that $f_{BB} - f_{BW} + f_{WW}$ is accidentally small and have a look on the remaining constants. Fig. 8.6 shows us such dependence. We can see that f_{DW} gives the largest contribution.

In the previous analysis, we have set $\Lambda = 1$ TeV which is an approximate estimate of the new physics scale. In Fig. 8.7, we have plotted the dependence of the decay rate on the scale Λ . As one would probably expect, the effects of new physics become more significant with decreasing value of Λ .

A question also rises how big is the effect of one-loop reducible graphs (8.8). Figure 8.8 shows that such effect is rather small, although not entirely negligible.

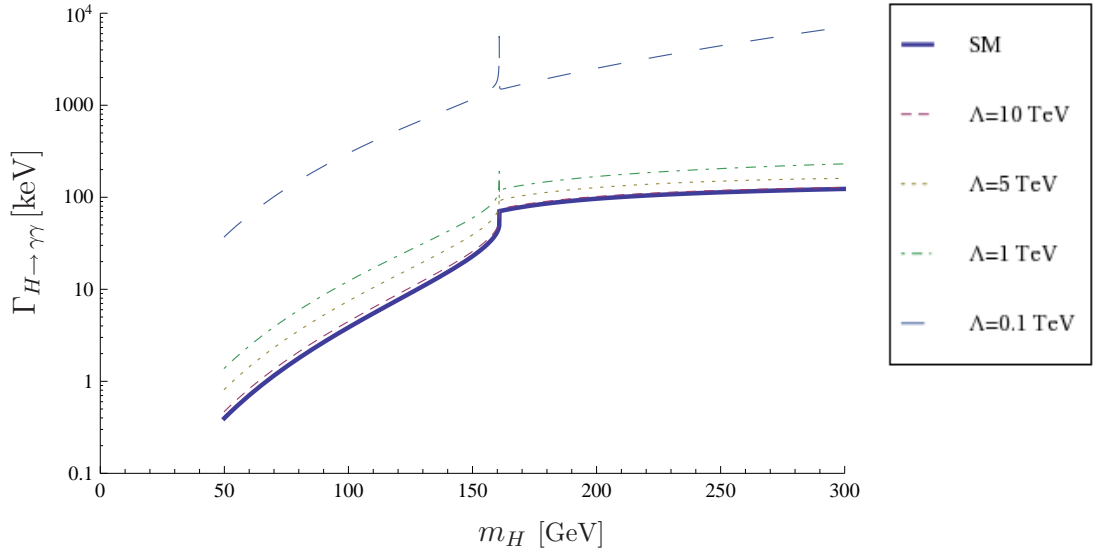


Figure 8.7: *Dependence of the new physics on the scale Λ . All f_i 's are set equal to 1.*

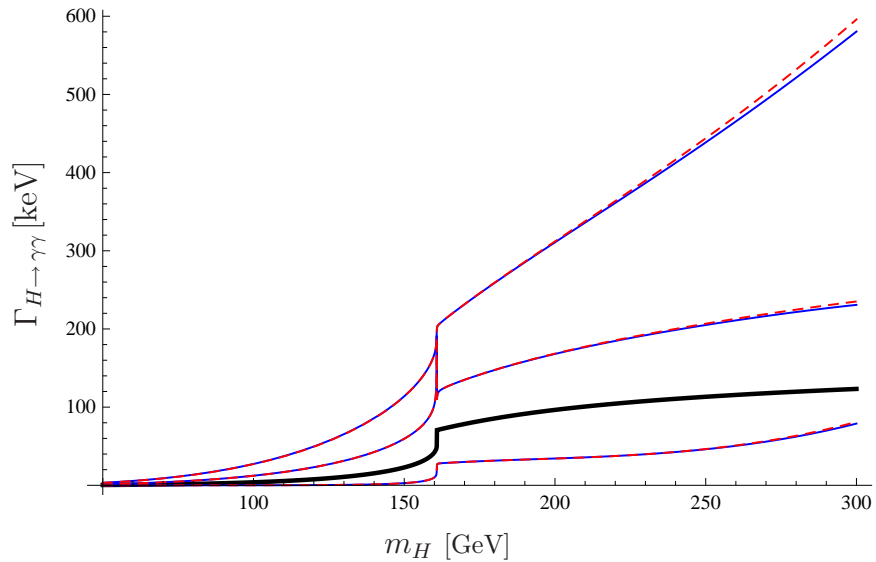


Figure 8.8: *Effect of one-loop reducible graphs: Thick curve is for SM, 3 sets of overlapping curves symbolize 3 sets of f_i choices, solid curves represent ignoring reducible graphs, dashed curves show calculations with reducible graphs included.*

8.2 Conclusion

We have examined electroweak processes in the framework of effective field theory (using effective Lagrangian approach), namely the process of decay $H \rightarrow \gamma\gamma$. An assumption that the new physics is characterized by mass scale $\Lambda \gg v$ has been made. We have employed a complete set of dimension-six $SU(2) \times U(1)$ invariant operators also invariant under charge conjugation and parity. Using this effective Lagrangian approach, we have evaluated tree-level and one-loop level correction to the well known SM result of $H \rightarrow \gamma\gamma$ decay and we have implemented a full renormalization within the framework of the effective theory. Possible issues that may arise during renormalization of such theory have also been discussed. We have discovered that contribution originating from dimension-six operators can significantly alter the original SM results. It is clear that the leading contribution within the domain of dimension-six operators comes from tree-level diagrams, but we have shown that one-loop diagrams involving dimension-six operators can play a significant role as well, given a proper value of the coupling parameters f_i . Plots for several different sets of constants f_i also suggest that for lighter Higgs, tree-level might dominate absolutely. Test of several random parameter sets f_i clearly indicates that the effects of new physics would more likely boost the original $H \rightarrow \gamma\gamma$ decay rate predicted by the SM, however, careful choice of f_i implies that it could also reduce it significantly. Detailed analysis of individual constants f_i shows that some of these parameters have stronger impact than the others. We have also shown the sensitivity of the new physics to the scale Λ : for the magnitude of $\Lambda = 10$ TeV, its effects almost diminish, while for 1 TeV and smaller, are strongly noticeable. Finally, some realistic assumptions about parameters f_i could be made, based on analysis of various other physical processes; however, such analysis would exceed the extent of this work. In this matter, we refer to [12].

Appendix A

Loop integrals

In evaluating loop integrals we have used the so-called Passarino-Veltman reduction [13], i.e. the reduction of tensor one-loop integrals to the special scalar integrals which can be further expressed by means of some standard analytical functions. In the text, we have employed the scalar integrals B_0 , C_0 and D_0 defined within dimensional regularization scheme as:

$$i\pi^2 A_0(m) = \int \frac{d^d l}{(2\pi\mu)^{d-4}} \frac{1}{[l^2 - m^2]}, \quad (\text{A.1})$$

$$i\pi^2 B_0(p_1^2, m_1^2, m_2^2) = \int \frac{d^d l}{(2\pi\mu)^{d-4}} \frac{1}{[l^2 - m_1^2][(l + p_1)^2 - m_2^2]}, \quad (\text{A.2})$$

$$i\pi^2 C_0(p_1^2, (p_1 - p_2)^2, p_3^2; m_1^2, m_2^2, m_3^2) = \int \frac{d^d l}{(2\pi\mu)^{d-4}} \frac{1}{[l^2 - m_1^2][(l + p_1)^2 - m_2^2][(l + p_2)^2 - m_3^2]}, \quad (\text{A.3})$$

$$i\pi^2 D_0(p_1^2, (p_1 - p_2)^2, (p_2 - p_3)^2, p_3^2, p_2^2, (p_1 - p_3)^2; m_1^2, m_2^2, m_3^2, m_4^2) = \int \frac{d^d l}{(2\pi\mu)^{d-4}} \frac{1}{[l^2 - m_1^2][(l + p_1)^2 - m_2^2][(l + p_2)^2 - m_3^2][(l + p_3)^2 - m_4^2]}. \quad (\text{A.4})$$

The C_0 and D_0 are UV finite, while B_0 is UV divergent for $d = 4$. Defining

$$\frac{1}{\tilde{\varepsilon}} = \frac{2}{4-d} - \gamma_E + \log 4\pi,$$

we have

$$A_0(m^2) = -m^2 \left(-\frac{1}{\tilde{\varepsilon}} - 1 + \log \frac{m^2}{\mu^2} \right) + O(\varepsilon) \quad (\text{A.5})$$

$$B_0(p^2, m^2, m^2) = \frac{1}{\tilde{\varepsilon}} - \log \frac{m^2}{\mu^2} + 2 + \sqrt{1 - 4\frac{m^2}{p^2}} \log \frac{\sqrt{1 - 4\frac{m^2}{p^2}} - 1}{\sqrt{1 - 4\frac{m^2}{p^2}} + 1}. \quad (\text{A.6})$$

One of the three-point functions used in (5.56) is given by

$$C_0(m_H^2, 0, 0; m_W^2) \equiv C_0(m_H^2, 0, 0; m_W^2, m_W^2, m_W^2) = -\frac{1}{m_H^2} \left[\text{Li}_2\left(\frac{2}{1 - \sqrt{1 - 4m_W^2/m_H^2}}\right) + \text{Li}_2\left(\frac{2}{1 + \sqrt{1 - 4m_W^2/m_H^2}}\right) \right], \quad (\text{A.7})$$

where $\text{Li}_2(x)$ is the standard dilogarithm defined through the Spence's integral:

$$\text{Li}_2(x) = -\int_0^x \frac{\log(1-t)}{t} dt. \quad (\text{A.8})$$

Further, let us denote

$$\begin{aligned} C_0(m_H^2, m_H^2, 0; m_W^2) &\equiv C_0(m_H^2, m_H^2, 0; m_W^2, m_W^2, m_W^2), \\ D_0(m_H^2; m_W^2) &\equiv D_0(m_H^2, 0, 0, 0, 0; m_W^2, m_W^2, m_W^2, m_W^2), \\ D_0(m_H^2, m_H^2; m_W^2) &\equiv D_0(m_H^2, m_H^2, 0, 0, 0, 0; m_W^2, m_W^2, m_W^2, m_W^2). \end{aligned}$$

A particular linear combination of these quantities appears in the last two lines of eq. (5.56). The resulting expression comes out to be quite simple, namely:

$$\begin{aligned} 2m_W^2 (D_0(m_H^2; m_W^2) + 2D_0(m_H^2, m_H^2; m_W^2)) (m_H^2 - 6m_W^2) - C_0(\dots) (m_H^2 + 6m_W^2) \\ = \frac{6(m_H^2 - 2m_W^2)}{m_H \sqrt{4m_W^2 - m_H^2}} \arctan\left(\frac{m_H}{\sqrt{4m_W^2 - m_H^2}}\right), \quad (\text{A.9}) \end{aligned}$$

as mentioned in [3]. Note finally that the proper analytic continuation of the above functions is obtained by means of the prescription $m^2 \rightarrow m^2 - i\varepsilon$ wherever it is necessary.

Bibliography

- [1] R. Barate *et al.* [ALEPH Collaboration], Phys. Lett. B **565** (2003) 61 [arXiv:hep-ex/0306033].
- [2] L. J. Hall, *Beyond the standard model*, ICHEP 2000, Osaka, Japan, 27 Jul - 2 Aug 2000.
- [3] J. Hořejší and K. Kampf, Mod. Phys. Lett. **A19** (2004) 1681-1694 [arXiv:hep-ph/0402147v2].
- [4] K. Kampf, *Effective field theories for Electroweak and Strong interactions*, Doctoral thesis, Prague 2004
- [5] J. Wudka, Int. J. Mod. Phys. A **9** (1994) 2301 [arXiv:hep-ph/9406205].
- [6] J. Hořejší: *Fundamentals of Electroweak Theory* (Karolinum Press, Prague 2002).
- [7] J. M. Hernandez, M. A. Perez and J. J. Toscano, Phys. Rev. D **51** (1995) 2044; M. A. Perez, J. J. Toscano and J. Wudka, Phys. Rev. D **52** (1995) 494 [arXiv:hep-ph/9506457].
- [8] K. Hagiwara, S. Ishihara, R. Szalapski and D. Zeppenfeld, Phys. Rev. D **48** (1993) 2182.
- [9] W. Buchmüller and D. Wyler, Nucl. Phys. B **268** (1986) 621.
- [10] D. Y. Bardin and G. Passarino: *The Standard Model In The Making: Precision Study Of The Electroweak Interactions* (Clarendon Press, Oxford 1999).
- [11] M. E. Peskin and D. V. Schroeder: *An Introduction to Quantum Field Theory* (Addison-Wesley Publishing Company, 1996).
- [12] B. Zhang, Y. P. Kuang, H. J. He and C. P. Yuan, Phys. Rev. D **67** (2003) 114024 [arXiv:hep-ph/0303048].
- [13] G. Passarino and M. J. Veltman, Nucl. Phys. B **160** (1979) 151.